UNIVERSITÀ DEGLI STUDI DI PADOVA

DIPARTIMENTO DI INGEGNERIA CIVILE, EDILE E AMBIENTALE

Department of Civil, Environmental and Architectural Engineering

Master in Water and Geological Risk Engineering

Analisi del trasporto solido in sospensione nel Fiume Po tra il 2009 e il 2019

Analysis of the suspended load in the Po River over the period 2009-2019

Relator:

Chiar.mo PROF. NICOLA SURIAN

Correlatori:

DOTT. ANDREA BRENNA

PROF. SIMONE BIZZI

Laureando:

BRYAN DALL'AGLIO

Matricola

2063147

ACADEMIC YEAR 2023-2024

Contents

List of Figures

List of Tables

1 Introduction

One of the most significant aspects of river morphodynamics is the cycle of sediment transport, as it is intricately linked to the river's morphology (Church, 2006), which subsequently influences the hydrodynamics of water motion controlling sediment transport. These factors collectively impact the biota of the river. Sediments originate from the weathering of exposed rocks (Bridge, 2003), the erosive effect of the river's water flow on the bed and banks of the channel, as well as glacial and snow melting processes. The fluvial sediment transport process comprises three phases (Pähtz et al, 2020): erosional entrainment, which marks the initiation of sediment movement into the fluid through fluid-induced stresses and bed forces; sediment transport, involving the movement of solid particles via momentum transfer between the fluid and sediment; and deposition, which entails the settling of organic and inorganic materials back onto the bed due to gravity (Garcia, 2008). The movement, entrainment, and deposition of suspended sediments are influenced by flow turbulence, particularly by an asymmetry between upward and downward velocity components of the turbulence (Parson et al., 2015; Bai et al., 2013).

Sediment movement in rivers can occur through two primary modalities: bedload and suspended load. Bedload transport primarily involves coarse material (i.e., cobble, gravel, sand), which glide, roll, and saltate along the streambed due to fluid drag force and gravity (Garcia, 2008). In contrast, suspended load primarily consists of fine material (i.e., sand, silt, clay), exhibiting irregular movements at indefinite heights in the water column (Bagnold, 1973); direct measurement of sediment concentration and water velocity is typically necessary to assess the suspended load. Sediment transport encloses both suspended sediment and bed load movement, although the majority of the total load in most large alluvial rivers, at least 85%, consists of suspended load (Babìnski, 2005).

The transport of sediment in a river is governed by various factors, including hydraulic factors related to flow characteristics, sediment characteristics such as dimensions and cohesion (Rodrigues et al, 2012), channel morphology including channel slope and roughness, climatic factors such as precipitation, and human activities such as land cover and channel modifications (Wilkes et al, 2018). Consequently, the motion of

particles in the river as suspended load exhibits significant temporal and spatial variability. Temporal variability is associated with the river's hydrological regime, precipitation factors (De Girolamo et al., 2015), and changes in the basin environment due to natural factors and human activities (Yang et al, 2002). The hydrological regime concerns floods, overland flow, and seasonality patterns, while human activities entail land use changes, deforestation, and alterations in the hydrological regime due to human channel interventions (Vercruysse et al, 2017). Natural factors include geomorphic processes (e.g. landslides), geological phenomena (e.g. volcanic eruptions), and ecosystem dynamics (e.g. vegetation growth). Spatial variability is linked to the geographic characteristics of the basin, where geological formations, climate, and land use play pivotal roles. For example, arable land is more susceptible to erosion due to vegetation loss, whereas forested areas are less prone to erosion due to better soil infiltration capacity (Panagos, 2015; Vercruysse et al, 2017). Moreover, mountainous rivers tend to transport more sediment compared to lowland rivers, and rivers surrounded by soft rock like siltstone carry a greater sediment load compared to those surrounded by hard rock like granite (Milliman, 2001). Channel morphology also influences sediment transport patterns, as different channel shapes exhibit distinct sediment transport behaviors (Pitlick et al, 2012).

The movements of suspended material are significant for the well-being of rivers. They not only significantly shape and control the geomorphological features of rivers and their fluvial landscape but also profoundly impact ecological communities, habitats, and nutrient transport (Vercruysse et al., 2017). This significance arises from the relationship between suspended sediment and turbidity, with turbidity serving as an indicator of water clarity and quality (Sader, 2017).

To delve into specifics, suspended sediment often carries organic matter and nutrients crucial for the flora and fauna of rivers. Moreover, it alters the physical and chemical properties of the water. Excessive sediment in the water column adversely affects river water quality, harming flora and fauna. High turbidity reduces sunlight penetration for submerged plants, elevates water temperature, and depletes oxygen levels (Larsen et al., 2010). Insufficient sediment intake is often anthropogenic, resulting in reduced nutrient transport and alterations in river morphology and its surrounding environment (Fondriest Environmental, Inc., 2014). Intense sedimentation can also diminish habitats

for aquatic animals and fish. Furthermore, suspended material may transport pollutants and heavy metals through particle binding (Walker et al, 2003).

Understanding sediment transport aids in assessing the damage associated with sediments during flood events (Vázquez-Tárrio et al, 2024) and their potential to obstruct hydraulic infrastructures (although such events are primarily related to bedload and vegetation transport). Given these implications of suspended sediment transport, and sediment transport in rivers more broadly, it stands as a pivotal consideration in river water and flood risk management (Nones et al., 2019).

This study aims to investigate the controlling factors of suspended sediment transport (*SST*) in the Po River over a decade extending from 2009 to 2019. The analysis concerns the entire basin, focusing on four stations along the Po River where data of *SST* are available: Piacenza, Cremona, Boretto and Pontelagoscuro. Additionally, twenty-one different tributaries were considered for water discharge. Specifically, eleven Alpine tributaries (Stura, Malone, Orco, Dora B., Sesia, Tanaro, Ticino, Lambro, Adda, Oglio, Mincio) and ten Apennine tributaries (Scrivia, Tidone, Trebbia, Nure, Arda, Taro, Parma, Enza, Secchia, Panaro) were studied.

The research hypotheses underlying the analysis are as follows:

1. Is it possible to differentiate between the contributions of Apennine tributaries and Alpine tributaries to the suspended sediment transport of the Po River?

2. Does water turbidity show seasonality and/or specific temporal patterns over the study period?

For the analysis, water discharge data and specific turbidity data were used. Water discharge refers to the volume of water flowing through a cross-section in a unit of time expressed in m^3/s. Specific turbidity is the ratio between turbid discharge and water discharge, indicating the concentration of sediment in the water column in kg/m^3.

2 Study area

2.1 General settings

The Po River is the longest watercourse in Italy, stretching 652 km in length, and boasting a catchment area of 70,091 km² at the Pontelagoscuro station (Figure 1), making it the largest basin in the country. Bounded by the Alps to the north and the Apennines to the south, the Po watershed comprises tributaries originating from these two distinct mountain ranges, which significantly influence its hydrology.

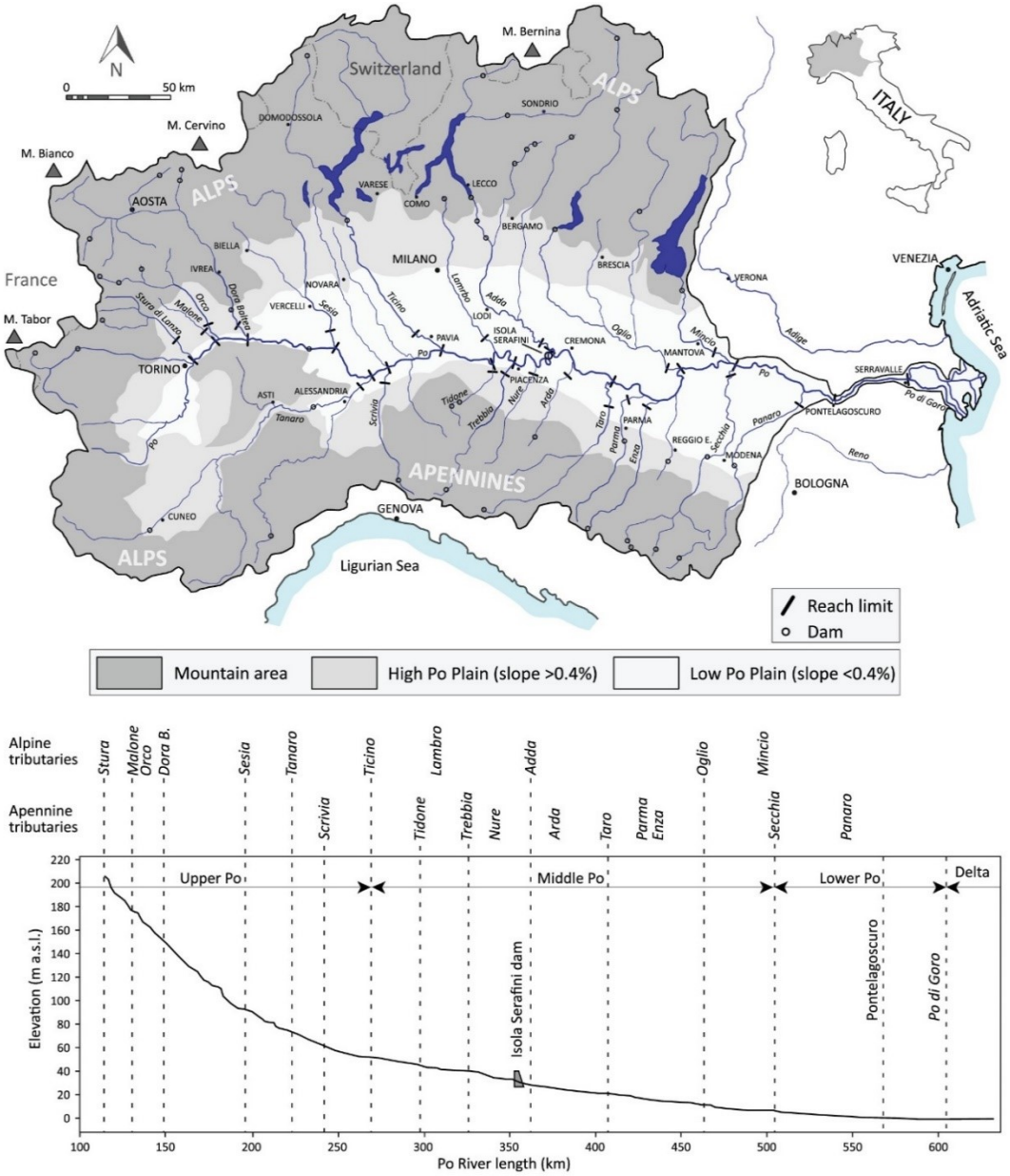

Figure 1. The Po River basin along with the tributaries taken into consideration in this work (from Brenna et al, 2022)

The Po River exhibits an averaged discharge of 1,500 m³/s at Pontelagoscuro (Zanchetti et al., 2008), with a runoff coefficient of 0.6. The maximum recorded discharge until 2012 reached 10,300 m³/s (Montanari, 2012). Notably, the Po River has experienced numerous floods over the past century, with 17 significant events recorded in: 1926, 1928, 1937, 1945, 1949, 1951, 1953, 1957, 1959, 1966, 1968, 1976, 1977, 1986, 1993, 1994, and 2000, the most severe of which occurred in 1951 (Montanari, 2012). The mean daily discharge time series from 1986 to 2003 is shown in Figure 2.

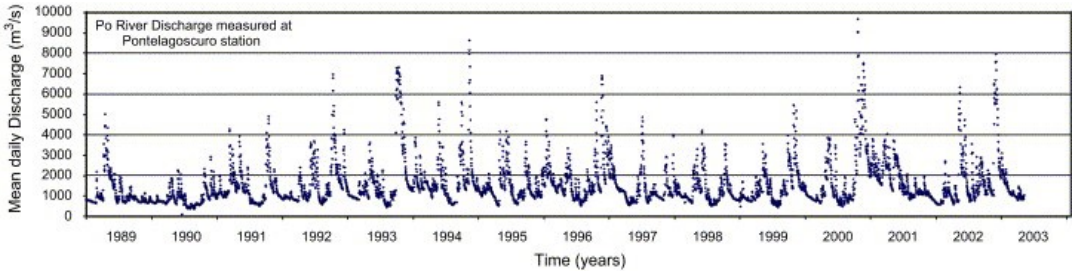

Figure 2. Mean daily discharge at Pontelagoscuro from 1986 to 2003 (from Syvitski & Kettner, 2007).

The precipitation across the basin varies significantly from one area to another (Figure 3), totaling an annual volume of 78 km³, with a mean annual value of 1080 mm recorded over the period from 1923 to 2008.

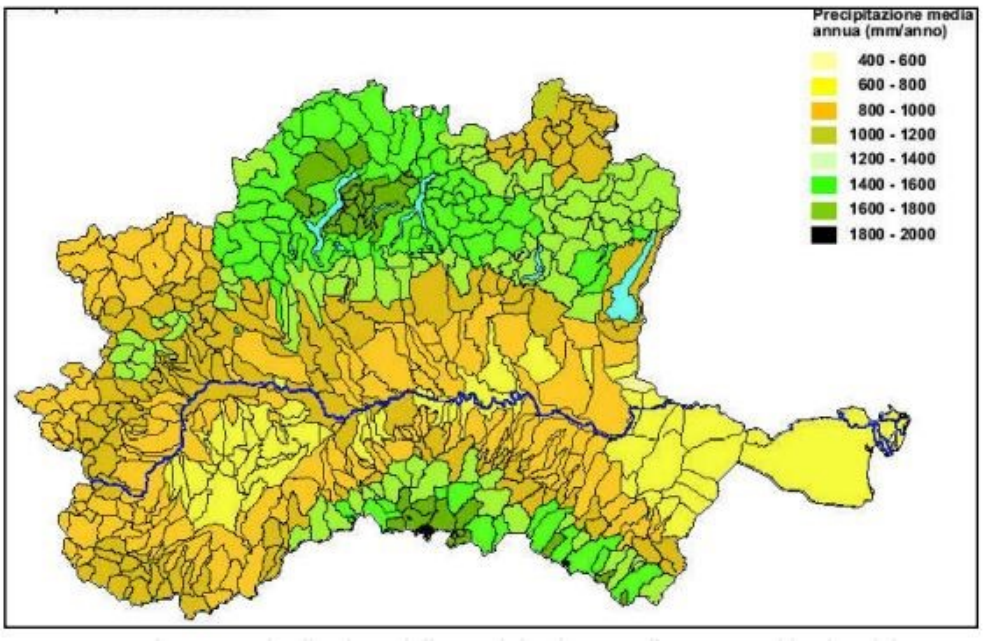

Figure 3. Distribution of the mean annual precipitation in the Po River basin, last updated in 2016 (from Autorità del bacino del fiume Po, 2016).

From Figure 3, it is evident that the highest precipitation is concentrated in the mountain areas of Alps and southern in Emilia-Romagna Region, while the lowest values are found in the Delta area and in the southwestern regions. In terms of hydrology, the 78 km^3 of precipitation are allocated as follows: approximately 20-25 km^3 for evapotranspiration, 9 km^3 to the aquifer, 1 km^3 for deep percolation, 5 km^3 for industrial use, 17 km^3 for irrigation purposes, and 6.5 km^3 extracted from the aquifer, posing a risk of overexploitation of underground water resources (Montanari, 2012). Seasonal precipitation patterns strongly influence the hydrological behavior of the Po River. Typically, the river experiences two high discharge periods, one in spring and the other in fall, along with two low discharge periods in winter and summer. The first peak is primarily attributed to snow melting, while the second peak is mainly due to the intense precipitation during the fall (Cattaneo et al., 2003).

Historically, the Po basin has been an attractive area for settlement, particularly for industrial and agricultural purposes, resulting in a densely populated region with approximately 17 million inhabitants (Marchetti, 2002). Several major industrial Italian cities, such as Turin, Milan, and Parma, are situated within the basin, making it a significant economic center for the country. The main channel is primarily utilized for water extraction for agricultural fields and hydropower purposes (Montanari, 2012). The basin is even renowned for its complex and varied ecosystem, featuring wetlands, marshes, and deltaic habitats that support diverse vegetation and animal species. Consequently, effective water resource management is essential to safeguard and study the ecosystem of this watershed.

2.2 Sediment transport in the Po River basin

The Po River is the most significant sediment supplier to the Adriatic Sea, with a total sediment discharge estimated to be approximately equal to 15 million tons per year (Bever et al., 2009). It exhibits a mean annual suspended sediment yield between 1925 and 2019 of 202 t $km^{-2}yr^{-1}$ (Billi & Spalevic, 2022). At the delta, specifically in the Pila mouth, which discharges 73% of all sediment into the Adriatic Sea from the river, sediment composition consists of 23% sand, 70% silt, and 7% clay (Nelson et al., 1970).

Historically, the Po River has undergone significant morphological changes and alterations in sediment transport, primarily due to human intervention. Notably

impactful were mining activities from 1950s-1990s and the construction of the Isola Serafini Dam in 1964 (Brenna et al., 2022), which led to channel incision and narrowing, resulting in changes to the planform of some reaches (Autorità di bacino del fiume Po, 2008). Another significant factor was continuous land use changes during the 20th century, resulting in a decrease in suspended sediment from 50% to 20% (Brenna et al., 2024).

To delve further, the course of the Po River (Figure 1) can be divided into three distinct sectors characterized by different streambed sediment composition and gradients. In the upper Po (up to about the confluence with the Ticino), slopes reach up to 0,14%, with mostly coarse sediments present. The central part, extending to the entrance of the Secchia River, has a more moderate slope of around 0,02%, with medium sand being predominant. The lower slope zone, with slope gradients ranging from 0,01% to 0,003%, is also characterized by the presence of medium to fine sand (Brenna et al., 2022).

Sediment supply is heavily influenced by the surrounding environment, particularly the diverse lithological and morphological characteristics of the Alps and the Apennines. The Po River receives tributaries from both mountain ranges. The Apennines mainly consist of marine sedimentary rocks such as, sandstone, marlstone and clay creating the so called “flysch”, but is also possible to find dolomite and limestone (ISPRA, 2014), while the Alps, being an older mountain range, comprise marine sediment and continental crust (Tesi et al, 2013), including igneous rocks like granite, metamorphic rocks like gneiss and sedimentary rocks like limestone and dolomite (ISPRA, 2014). These geological differences result in distinct sediment inputs, with sediment production from the Apennine chain significantly higher than that from the Alps (Cattaneo et al, 2003). Apennine basins typically produce between 4 to 20 t/ha/yr, whereas Alpine basins generally produce less than 1 t/ha/yr, except in exceptional cases (Van Rompaey et al, 2005). In terms of specific turbidity, the Alpine rivers exhibit an average value of 0.22 kg/m^3, whereas the Apennine rivers show an average value of approximately 2.75 kg/m^3 (Raiteri, 1994), i.e., an order of magnitude higher than the one from the Alps. However, Alpine basins tend to have higher discharges than Apennine basins, particularly in the Po River the Apennine tributaries contribute only 15% to 20% of the water discharge but up to 80% of the suspended transport (Del

Longo, 2018). Previous studies on the Po River have identified three zones with different sedimentological and water inputs along the river. An analysis between 1971 and 1987 (Figure 4) revealed that the zone from the source up to Piacenza contributes 66% to the total runoff and 35% to the total sediment load. The zone between Piacenza and Boretto, particularly the Apennine zone, appears to be the most significant for sediment contribution, accounting for 56% of the sediment load and 20% of the runoff. From Boretto to the delta, the contribution is 14% for total runoff and 10% for total sediment load (Syvitski & Kettner, 2007).

Figure 4. Runoff (mm/month) and sediment load (kT/month) during the period 1971–1987 from three stations: Piacenza, Boretto, Pontelagoscuro (from Syvitski & Kettner, 2007).

Despite the information presented here, the regime of sediment fluxes of the Po River at the basin scale has only been partially studied (Vignati et al, 2003), often focusing on single-event timescales. This work aims to provide a deeper understanding of this process.

3 Data and Methods

3.1 Data

The data utilized in this study are primarily categorized into two types: water discharge and specific turbidity. Regarding the water discharges, a database was compiled concerning the average daily water discharges from 2009 to 2019 of the twenty-one considered tributaries (refer to Table 1). The selected stations were those situated closest to the junction with the Po River. However, for certain streams such as the Oglio and the Lambro rivers, there was a data deficiency exceeding 50 percent, while tributaries from Emilia Romagna lacked data for the entirety of 2019. Data were sourced from the portals of ARPA Piemonte (https://www.arpa.piemonte.it/rischi_naturali/snippets_arpa_graphs/map_meteoweb/?rete=stazione_meteorologica), ARPA Lombardia (https://idro.arpalombardia.it/it/map/sidro/), and ARPA Emilia-Romagna (https://simc.arpae.it/dext3r/). Concerning water discharges in the Po River, data were provided by the Po River Basin Authority (AdbPo) for the four hydrometric stations located in Piacenza, Boretto, Cremona, and Pontelagoscuro (Figure 5).

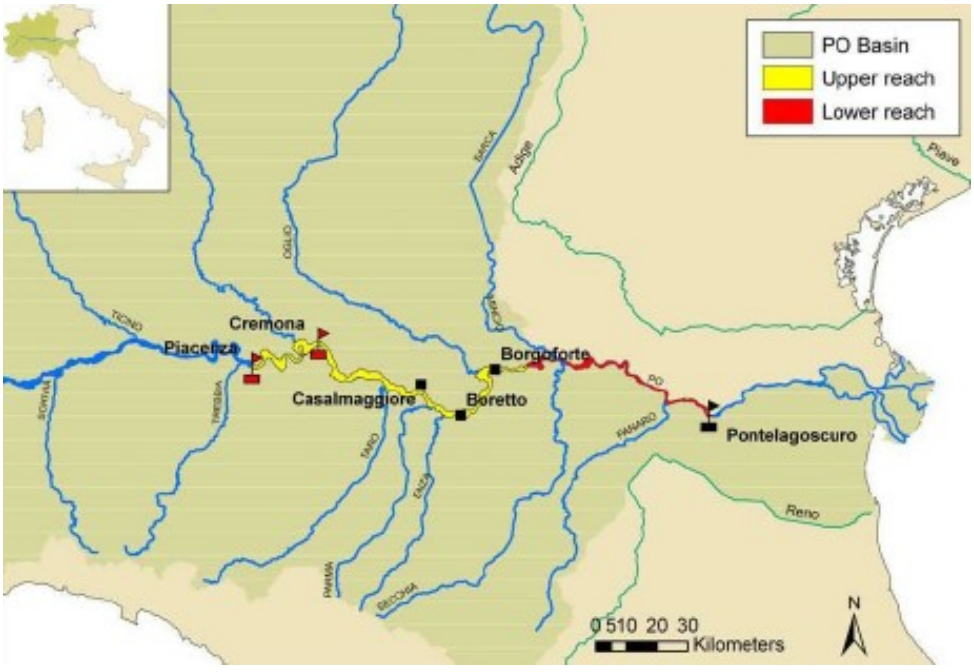

Figure 5. Location of the four hydrometric stations: Piacenza, Cremona, Boretto and Pontelagoscuro (from Domeneghetti et al, 2011)

Table 1. The names of the locations for the gauging stations on each tributary.

Tributary	**Station's name**
Dora Baltea	Verolengo
Malone	Brandizzo
Orco	San Benigno
Sesia	Palestro
Stura	Torino
Tanaro	Montecastello
Adda	Lodi
Lambro	Salerano Sul Lambro
Mincio	Ponti Sul Mincio
Oglio	Marcaria
Ticino	Vigevano
Scrivia	Guazzora
Arda	Fiorenzuola D'Arda
Parma	Parma Ponte Verdi
Taro	S.Secondo
Enza	Sorbolo
Nura	Pontenura
Panaro	Bomporto
Secchia	Ponte Bacchello
Tidone	Rottofreno
Trebbia	Rivergaro

Suspended sediment transport data were also provided by AdBPo and are also available in the hydrological Annals (https://www.arpae.it/it/temi-ambientali/meteo/report-meteo/annali-idrologici; https://www.adbpo.it/open-data/). In hydrological annals, data are available on a monthly scale, providing averages, maximums, and minimums. Conversely, the data provided by AdBPo are on a daily scale. They are expressed in specific turbidity and potentially in turbid discharge; however, for the purposes of this study, only the former was utilized. The database pertaining to these data is relatively comprehensive; nevertheless, some entries seemed to be interpolated based on measurements from the preceding and succeeding days. These interpolations were excluded, and only data reflecting direct measurements of suspended sediment were incorporated for analysis. It is important to note that there are specific methodologies for correctly sampling sediments in the water column. The ideal approach involves conducting multiple systematic samplings to obtain a weighted average and derive a representative value for the river at the defined section. However, this method can be

costly and time consuming, so typically, a sampling area is selected that is deemed representative of the watercourse. Typically, a point just below the water surface within the main stream of the river is chosen for sampling (ISPRA, 2010). There are various samplers available for this purpose, with the Giandotti sampler (Figure 7) being the one commonly used by ARPA-E up to 2018. These samplers typically employ filters designed to capture a certain range of sediment sizes. Subsequently, after sieving and weighing of sediments, specific turbidity values are obtained. In the case of samples taken along the Po River, as utilized in this study, samples were collected from the uppermost layer of the water column. Therefore, the data primarily comprise wash loads, representing the smallest fraction of suspended sediments that are unlikely to deposit. These particles are not typically represented in the streambed (Church, 2006) and are mainly associated with hillslope runoff during periods of intense precipitation (Khullar, 2007). It is possible to gain a deeper understanding of how the wash load contributes to suspended sediments by referring to Figure 6. This figure illustrates the classification based on the transport method, where the suspended sediment load is composed of the combined total of the suspended bed-material load and, the wash loads.

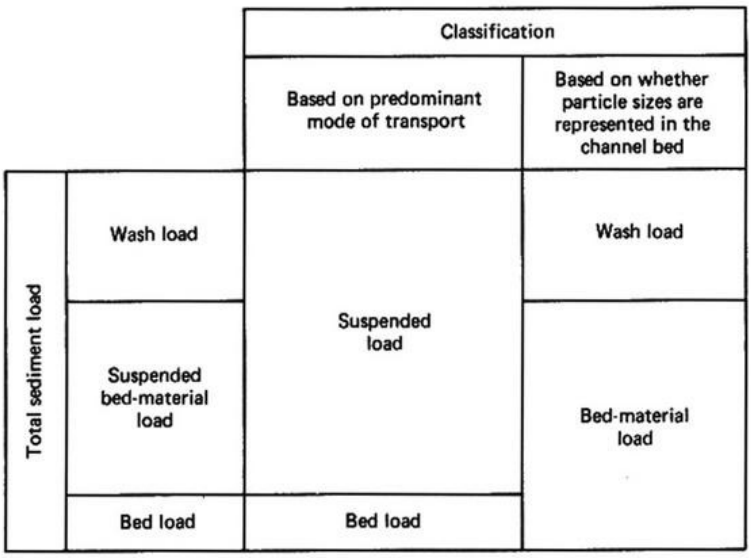

Figure 6. Classification of sediment load based on mode of transport and on whether particle sizes are represented in the channel bed (from Ponce, n.d.).

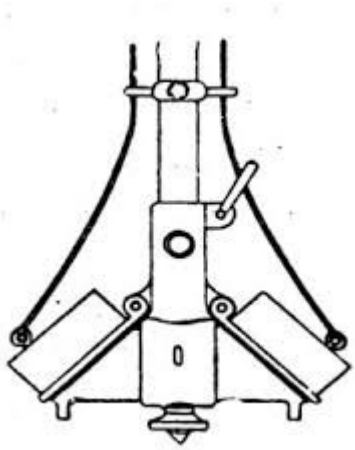

Figure 7. Design of the Giandotti sampler.

3.2 Methods

This study aims to investigate the controlling factors of sediment transport in the Po River from 2009 to 2019. The research was divided into two parts. The first part aimed to examine the contribution of Apennine and/or Alpine tributaries to suspended sediment transport in the Po River. Initially, this analysis used a parameter that correlated the water discharges of the Apennine and Alpine tributaries with turbidity in the Po River. Subsequently, the analysis became more rigorous through the creation of duration curves for all tributaries and the application of Pearson's coefficient.

The second part of the analysis aimed to identify seasonality in suspended sediment transport or at least a temporal pattern. This analysis was conducted by studying the year-by-year time series and, subsequently, by using box plots to represent specific turbidity and water discharges in different months of the year.

3.2.1 Analysis of the contribution of Alpine and Apennine tributaries

Historically, it is known that the Apennine rivers tend to have higher sediment transport rates than the Alpine ones (Raiteri, 1994; Van Rompaey et al., 2005), especially in the Po River catchment, where the Apennine tributaries contribute 15% to 20% of the water discharge but up to 80% of the suspended load of the Po River (Del Longo, 2018). Based on this knowledge, a series of analyses were conducted to observe whether certain values of water discharge in the Apennine and/or Alpine tributaries led to specific behaviors in the values of specific turbidity.

The first step for this analysis involved plotting in Microsoft Excel specific turbidity as a function of water discharge for the four stations along the Po River. Additionally, a database in Microsoft Excel containing discharge data for the twenty-one tributaries, categorized into Apennine and Alpine tributaries was created. Subsequently, a ratio, called the Alpine-Apennine Flow Index (*AAFI*) (1), was calculated between the water discharge values in the Apennine rivers and the discharge values in the Alpine rivers for the stations of Pontelagoscuro and Piacenza.

In the *AAFI* calculation, flood event dates in the Po River with discharge values ranging from 2500 to 3100 m³/s were considered for the Pontelagoscuro station. Similarly, for the Piacenza station, data corresponding to water discharges between 1500 m³/s and 2300 m³/s were used. These ranges have been chosen to have values of flood slightly higher than the mean values of discharge for Piacenza and Pontelagoscuro that are respectively 959 m^3/s and 1490 m^3/s (Montanari, 2012).

$$AAFI = \frac{Q_{Alp}}{Q_{App}} \quad (1)$$

Where Q_{App} (m^3/s) represents the sum of discharge from all the Apennine tributaries, for the date considered plus four days before and the date considered plus two days before for Pontelagoscuro and Piacenza. Instead, Q_{Alp} (m^3/s) represents the sum of discharge from all the Alpine tributaries, respectively, for the date considered plus four days before for Pontelagoscuro and the date considered plus two days before for Piacenza. Considering the limited information on the time of concentration of the Po River, the selected time windows guarantee a comprehensive outflow of sediments to the designated closing station (in this case Piacenza or Pontelagoscuro).

Later, the analysis became more rigorous by creating a database of duration curves for all twenty-one tributaries under consideration in Microsoft Excel. The flow duration curve (FDC), being one of the best and most used methods to characterize flow regime and the hydrological behavior of a river, is a useful representation for determining the characteristics of flow in a river based on frequency analysis (Burgan & Aksoy, 2022). FDCs indicate the percentage of time (or frequency) during which a streamflow is equaled or exceeded during a certain period (Zhao et al, 2021). It is an alternative

representation of the cumulative distribution function of discharges (Yokoo & Sivapalan, 2011). To obtain the duration curves, it was necessary to arrange the discharge data of each tributary in descending order and then calculate the exceedance probability using the Weibull plotting position method (2).

$$\% \, EXC = \frac{m}{N + 1} \tag{2}$$

Where *%EXC* represents the percentage of exceedance for the value under consideration during the observation period of the data. *N* denotes the total number of data points, and *m* denotes the position of the data within the ordered series.

These curves are crucial for the subsequent analysis using the Pearson coefficient (*r*). The Pearson test is utilized to measure the correlation between two continuous quantities (Faizi & Alvi, 2023). This coefficient ranges from -1 to +1, where 0 indicates no correlation, -1 indicates inverse linear correlation, and +1 indicates direct linear correlation (Nettleton et al, 2014).

The idea behind calculating high absolute Pearson values in Excel is to indicate a possible linear correspondence between the duration curve (and therefore the water discharges) and specific turbidity. For this reason, a table with all Pearson values has been created. Pearson's coefficient has been calculated for both stations. The correlation has been studied between the duration curve and the specific turbidity for the same day considered, but also between the duration curve and the values of the following five days of the specific turbidity at Pontelagoscuro (indicated with t+1, t+2, t+3, t+4 and t+5). The same procedure was also applied to Piacenza station, with consideration given to the day of observation and the subsequent three days. As seen before for the calculation of the *AAFI*, these time windows ensure a complete outflow of sediments to the designated closing station (in this case Piacenza or Pontelagoscuro). The same scheme was also implemented between the logarithmic values of the specific turbidity and the duration curve and between both quantities taken as logarithmic. In particular, further analyses were conducted in MATLAB on the highest absolute values found respective to the Alpine and Apennine tributaries for both the Pontelagoscuro and Piacenza stations. Graphs were plotted with MATLAB that relate specific turbidity

at Pontelagoscuro and Piacenza with the water discharges of the chosen tributaries and also the water discharges in the river Po and/or the *AAFI*.

3.2.2 Analysis of time patterns and seasonality in the SST

The second part of the study involved examining the seasonality and potential temporal patterns between sediment transport and water discharges. The aim was to determine whether increases in specific turbidity values were directly influenced by peaks in water discharge, or if they corresponded to periods of low river discharge or snowmelt. This investigation focused exclusively on Pontelagoscuro, as it serves as the primary measuring station for basin closure. Thus, Pontelagoscuro is deemed representative of the overall behavior of the entire basin.

The analysis started by examining with Microsoft Excel three years with varying characteristics at the Pontelagoscuro station. Specifically, 2014 was a "wet" year characterized by lower specific turbidity values and significantly higher water discharge values, while 2016 exhibited opposite characteristics. The year 2010 was chosen as an intermediate reference. For these years, days with specific turbidity values exceeding 0.4 kg/m^3 were identified, and their corresponding periods and months were analyzed. Subsequently, time series data for Pontelagoscuro, including specific turbidity and water discharges, were analyzed to identify potential correspondences between discharge and turbidity peaks or other types of temporal patterns.

To enhance the rigor of the analysis, a series of box plots was generated with Statgraphics 19. The first set of box plots depicted the relationship between water discharges and specific turbidity values for the entire dataset, categorized by month of the year. The second set of box plots, consisted in a zoom of the first one and considered only the data above the 90^{th} percentile of specific turbidity and water discharge, again divided into monthly intervals for analysis. For discharges, this threshold corresponded to 2739.4 m^3/s, while for specific turbidity to 0.177 kg/m^3. As the final step of the study, a summary table was constructed with Microsoft Excel to present the average and median values derived from the box plots, along with the monthly ratios between them.

4 Results

4.1 Contribution of Alpine and Apennine tributaries to the suspended sediment transport in the Po River

The first elaboration made it possible to plot Figure 8 and Figure 9, in which the specific turbidity is related to the water discharge. Based on the concept that generally the Apennine rivers have more suspended sediment transport and less water discharge (Del Longo, 2018), it has been hypothesized the presence of three areas in which it was possible to distinguish a certain intake. In the orange zone, therefore the area related to low water discharges and high turbidity values, it was hypothesized that it could result from a greater Apennine tributaries contribution, Conversely, the blue zone was thought to indicate an area with a greater Alpine contribution given the high-water discharges and the specific turbidity values relatively low. The central area, the green one, however, was assumed to be an area where there was a contribution of the tributaries of both mountain ranges.

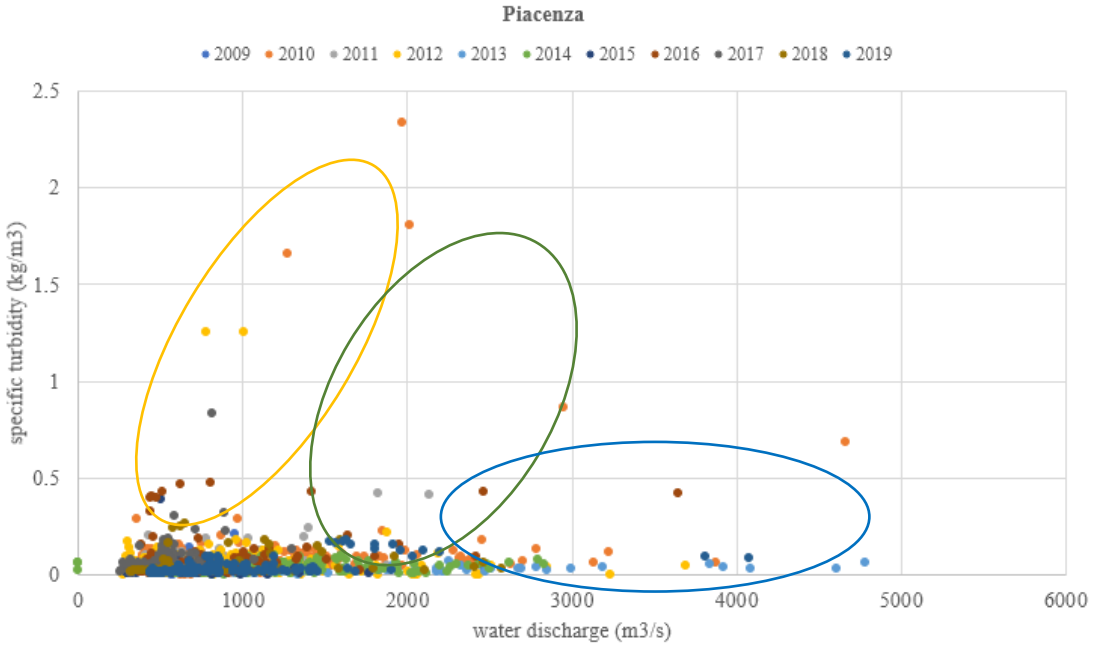

Figure 8. Relationship between specific turbidity (kg/m^3) and water discharge (m^3/s) for the Piacenza station.

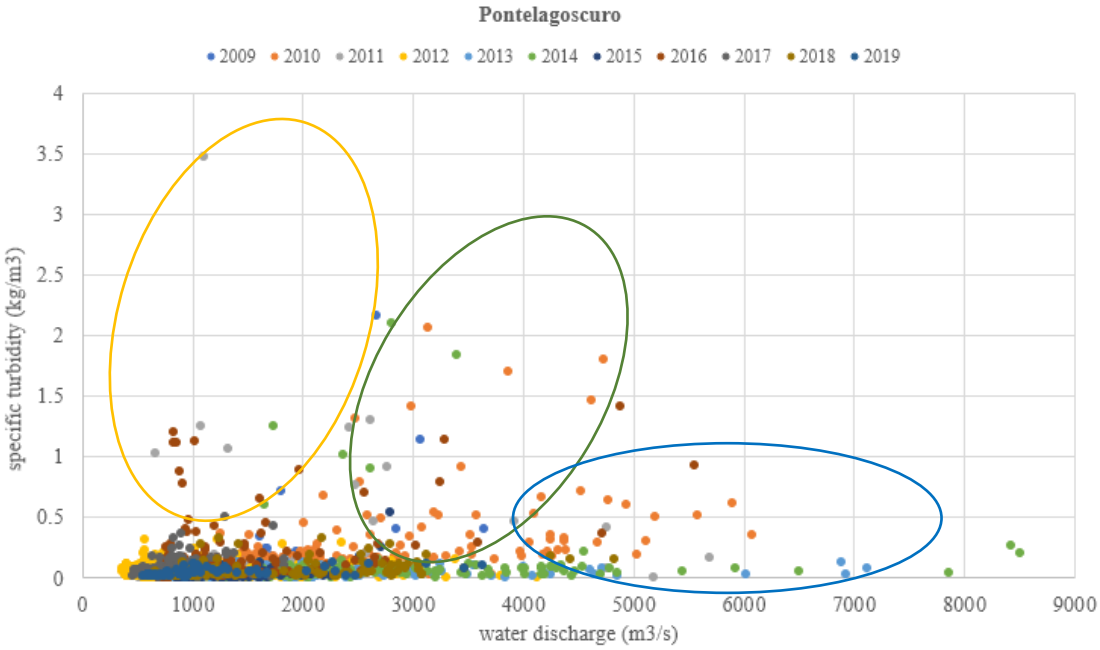

Figure 9. Relationship between specific turbidity (kg/m^3) and water discharge (m^3/s) for the Pontelagoscuro station.

The next step was the creation of the database with the water discharge time series (Figure 10) for the twenty-one tributaries divided between Apennine and Alpine for the 2009-2019 period.

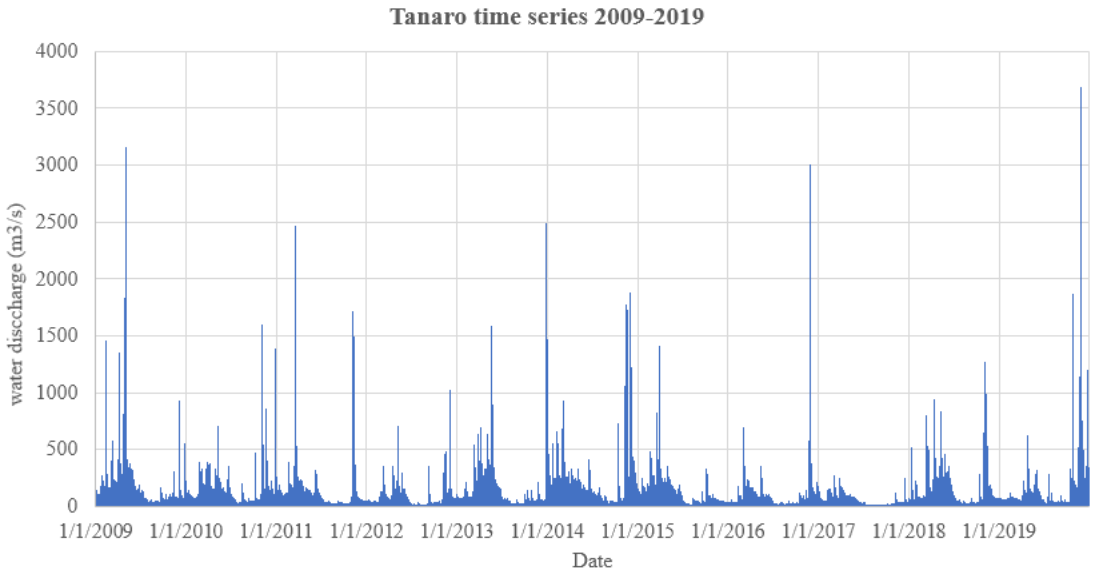

Figure 10. Example of time series extracted from the database. Tanaro mean daily discharge time series from 2009 to 2019.

Observing Figure 8 and Figure 9 has been chosen an interval in which to analyze point by point the values of specific turbidity. Such interval as mentioned above was ranging

between 2500 and 3100 m³/s for the Pontelagoscuro station, and between 1500 m³/s and 2300 m³/s for Piacenza station. Following the calculation of the *AAFI*, two graphs were obtained relating the specific turbidity to that index (Figure 11 and Figure 12).

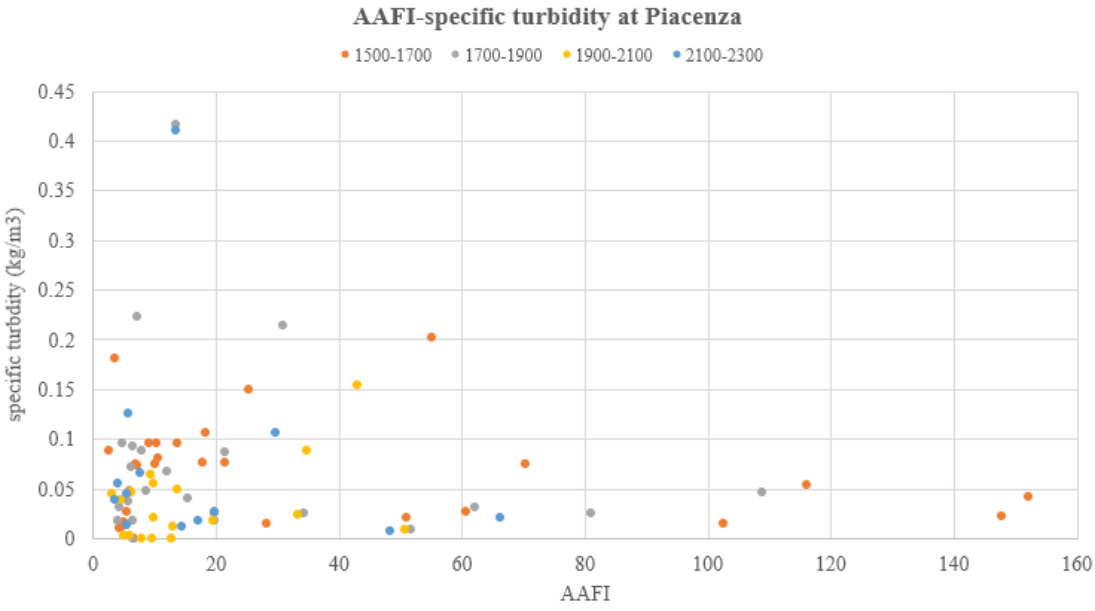

Figure 11. Relationship between specific turbidity (kg/m³) and AAFI for the Piacenza station.

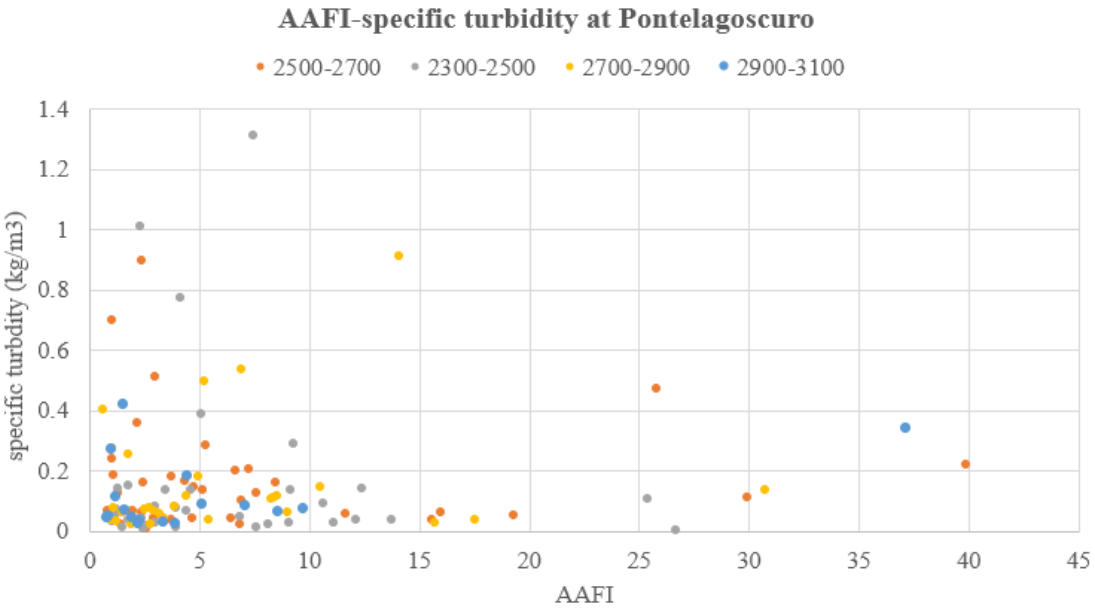

Figure 12. Relationship between specific turbidity (kg/m³) and AAFI for the Pontelagoscuro station.

In the graph relative to the Piacenza station (Figure 11) the values of turbidity have a range between 0.41 kg/m^3 and 0.0007 kg/m^3 with values of the AAFI up to 152. For the graph relative to Pontelagoscuro (Figure 12) instead the values of turbidity vary between 1.31 kg/m^3 and 0.002 kg/m^3 while the AAFI reaches a maximum of 40. In both Figure 11 and Figure 12, it is possible to observe, except for some points, an increase of the turbidity with a decrease of the value of the AAFI. This trend shows that during periods of high discharges in the Apennine rivers or potentially low water discharges in Alpine rivers, there is a notable rise in specific turbidity. Consequently, this results in an increase in the concentration of suspended sediment within the water column. For a more rigorous analysis of the correlation between the water discharge of the tributaries and the specific turbidity it was decided to use the coefficient of Pearson, however it was necessary to create an additional database with the duration curves for the tributaries (Figure 13 and Figure 14).

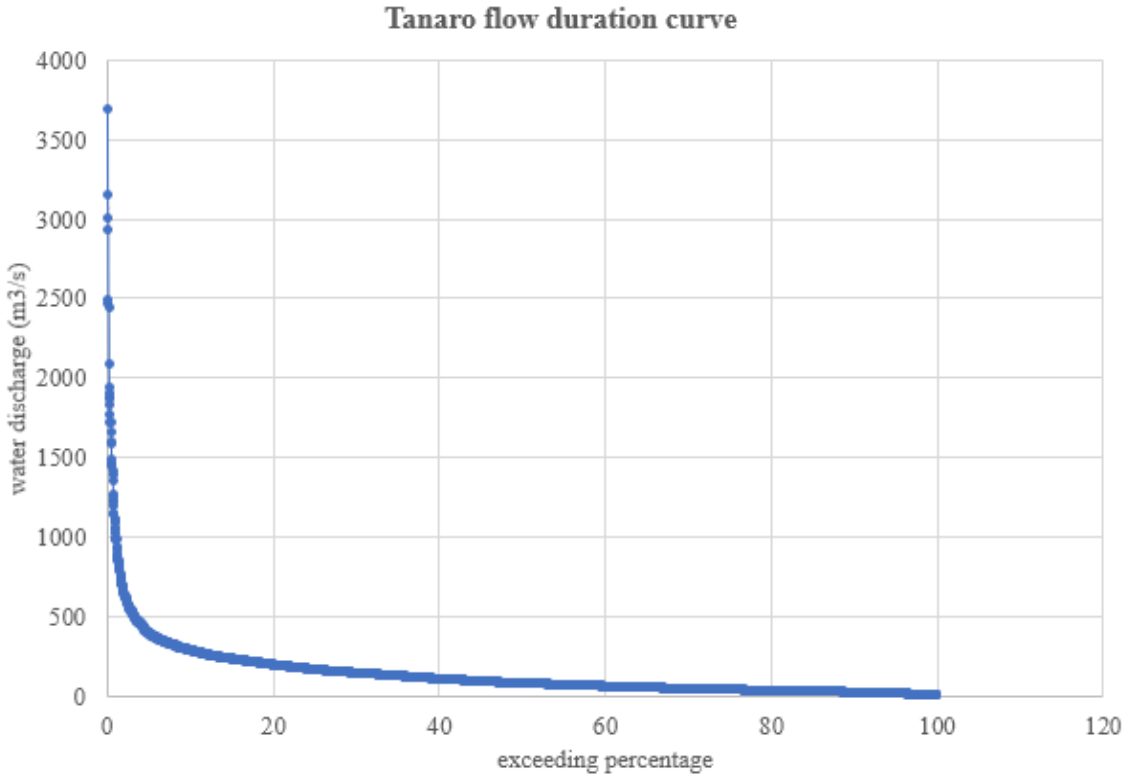

Figure 13. Example of flow duration curve extracted from2009-2019 time series for the. Tanaro River.

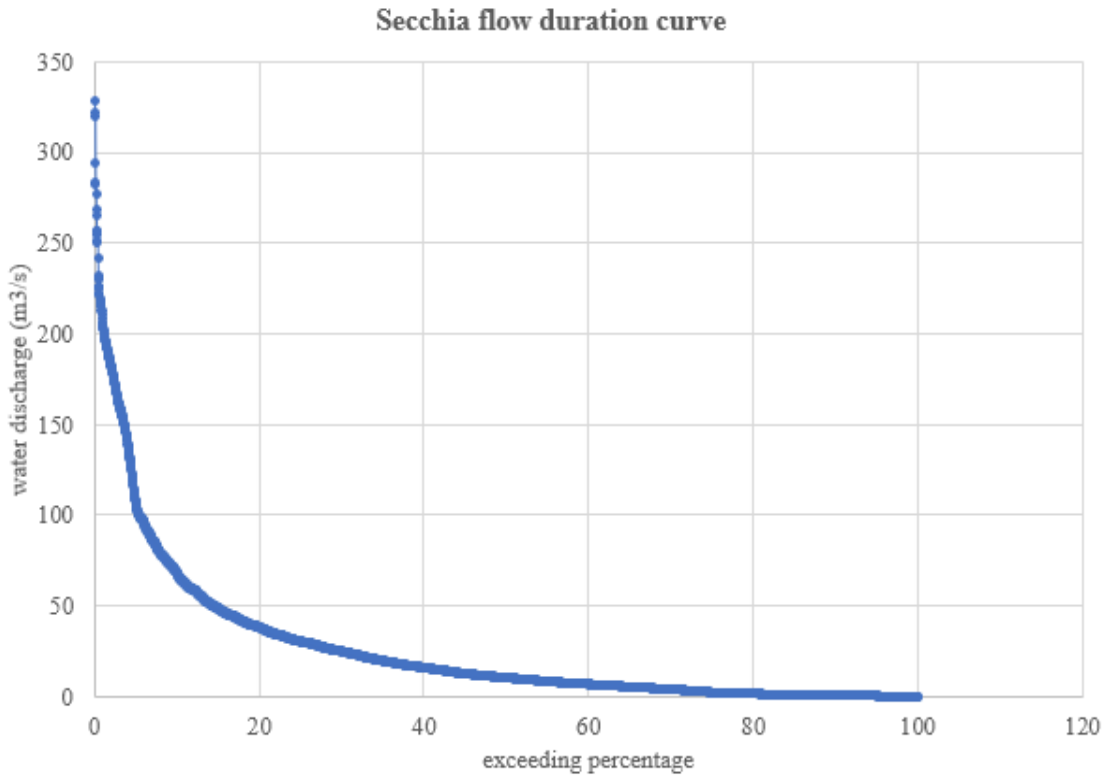

Figure 14. Example of flow duration curve extracted from2009-2019 time series for the. Secchia River.

Next, the Pearson coefficients were calculated. Table 2 presents the Pearson coefficients calculated between the specific turbidity measured at Pontelagoscuro and Piacenza and the duration curves of the various tributaries. The correlation has been studied for the same day considered, but also between the duration curve and the values of specific turbidity of the following five days at Pontelagoscuro (indicated with t+1, t+2, t+3, t+4 and t+5), and between the duration curve and the values of specific turbidity of the following three days at Piacenza (indicated with t+1, t+2, t+3). The same reasoning was applied in the calculation of Table 3, between the duration curves of the tributary and the logarithm of the specific turbidity, and in the calculation of Table 4 between the logarithm value of both duration curves and specific turbidity.

In all three tables (Table 2, Table 3 and Table 4), the highest absolute values for the two stations were then highlighted, distinguishing between contributions from Alpine and Apennine tributaries. In Table 2, the absolute values reach a maximum of around 0.2, indicating a weak correlation between specific turbidity at the two stations along the Po River and the duration curves of its tributaries, and therefore, their water discharges. Values close to approximately plus or minus 1 would have indicated a

strong statistical correlation among these quantities. However, one exception is noted with the Oglio River, which exhibits a slightly higher absolute value exceeding 0.4. The two highest absolute Pearson coefficient values for the Piacenza station are associated with the Tanaro for Alpine rivers and the Scrivia for the Apennine rivers. Conversely, for the Pontelagoscuro station, the highest absolute values are observed for the Oglio and Panaro rivers compared to both the Alpine and Apennine tributaries.

		PIACENZA				PONTELAGOSCURO					
		t	*t+1*	*t+2*	*t+3*	*t*	*t+1*	*t+2*	*t+3*	*t+4*	*t+5*
ALPS	*Stura*	-0.081	-0.084	-0.031	0.008	-0.120	-0.139	-0.138	-0.096	-0.037	-0.004
	Malone	-0.109	-0.105	-0.052	-0.024	-0.158	-0.175	-0.180	-0.127	-0.058	-0.025
	Orco	-0.045	-0.041	0.010	0.039	-0.071	-0.085	-0.083	-0.047	0.005	0.028
	Dora B.	-0.026	-0.019	0.011	0.030	-0.033	-0.052	-0.054	-0.015	0.030	0.047
	Sesia	-0.112	-0.089	-0.039	0.000	-0.185	-0.193	-0.194	-0.140	-0.078	-0.053
	Tanaro	-0.118	***-0.122***	-0.074	-0.032	-0.192	-0.196	-0.195	-0.149	-0.087	-0.056
	Ticino	-0.051	-0.049	-0.035	-0.027	0.033	0.018	0.005	0.004	0.025	0.024
	Lambro	0.001	0.005	-0.024	-0.022	-0.108	-0.127	-0.151	-0.115	-0.032	0.025
	Adda	NO	NO	NO	NO	-0.157	-0.156	-0.147	-0.114	-0.091	-0.075
	Oglio	NO	NO	NO	NO	-0.418	***-0.453***	-0.420	-0.418	-0.349	-0.343
	Mincio	NO	NO	NO	NO	0.023	0.028	0.025	0.024	0.020	0.026
APPENNINES	*Scrivia*	***-0.111***	-0.111	-0.048	0.012	-0.152	-0.153	-0.153	-0.126	-0.086	-0.067
	Tidone	-0.077	-0.066	-0.050	-0.044	-0.099	-0.113	-0.116	-0.075	-0.031	-0.019
	Trebbia	-0.078	-0.077	-0.028	0.001	-0.144	-0.136	-0.136	-0.112	-0.070	-0.056
	Nure	NO	NO	NO	NO	-0.087	-0.098	-0.116	-0.091	-0.049	-0.016
	Arda	NO	NO	NO	NO	-0.160	-0.167	-0.157	-0.117	-0.075	-0.073
	Taro	NO	NO	NO	NO	-0.145	-0.155	-0.165	-0.150	-0.105	-0.085
	Parma	NO	NO	NO	NO	-0.195	-0.211	-0.200	-0.142	-0.097	-0.085
	Enza	NO	NO	NO	NO	-0.140	-0.134	-0.116	-0.063	-0.046	-0.040
	Secchia	NO	NO	NO	NO	-0.216	-0.208	-0.177	-0.125	-0.101	-0.097
	Panaro	NO	NO	NO	NO	***-0.222***	-0.213	-0.191	-0.135	-0.102	-0.091

Table 2. Pearson coefficient values between specific turbidity in the Po River at Piacenza and Pontelagoscuro and water discharge in the tributaries. The highlighted values are the highest for each station respect to an Alpine and Apennine tributary.

In Table 3, the absolute values reach a maximum of around 0.2. However, also in this case, one exception is noted with the Oglio River, which exhibits a slightly higher absolute value exceeding 0.4. The two highest absolute Pearson coefficient values for the Piacenza station are associated with the Ticino for Alpine rivers and the Tidone for the Apennine rivers. Conversely, for the Pontelagoscuro station, the highest absolute values are observed for the Oglio and Panaro rivers compared to both the Alpine and Apennine tributaries.

		PIACENZA				PONTELAGOSCURO					
		t	*t+1*	*t+2*	*t+3*	*t*	*t+1*	*t+2*	*t+3*	*t+4*	*t+5*
ALPS	*Stura*	-0.0506	-0.0522	-0.0469	-0.0311	-0.1111	-0.1212	-0.1244	-0.1035	-0.0670	-0.0353
	Malone	-0.1058	-0.1149	-0.1795	-0.0982	-0.1692	-0.1798	-0.1789	-0.1516	-0.1108	-0.0751
	Orco	-0.0207	-0.0237	0.0488	-0.0048	-0.0776	-0.0852	-0.0859	-0.0678	-0.0340	-0.0084
	Dora B.	0.0483	0.0479	0.1207	0.0603	-0.0152	-0.0253	-0.0398	-0.0247	0.0012	0.0206
	Sesia	-0.0675	-0.0568	0.1076	-0.0117	-0.2128	-0.2236	-0.2253	-0.1927	-0.1512	-0.1248
	Tanaro	-0.1334	-0.1359	0.0253	-0.1100	-0.2428	-0.2485	-0.2494	-0.2228	-0.1802	-0.1455
	Ticino	-0.0634	-0.0528	***0.2078***	-0.0400	0.0112	0.0149	0.0177	0.0362	0.0576	0.0538
	Lambro	-0.0129	-0.0187	0.1245	-0.0287	-0.1111	-0.1181	-0.1378	-0.1190	-0.0696	-0.0299
	Adda	NO	NO	NO	NO	-0.1984	-0.2024	-0.1901	-0.1556	-0.1276	-0.1102
	Oglio	NO	NO	NO	NO	-0.4137	***-0.4888***	-0.4488	-0.4330	-0.3674	-0.3639
	Mincio	NO	NO	NO	NO	0.0462	0.0535	0.0515	0.0548	0.0384	0.0548
APPENNINES	*Scrivia*	-0.0699	-0.0668	0.1139	-0.0207	-0.1640	-0.1691	-0.1789	-0.1545	-0.1227	-0.1027
	Tidone	-0.0940	-0.0888	***0.1779***	-0.0801	-0.1034	-0.1195	-0.1219	-0.1054	-0.0771	-0.0550
	Trebbia	-0.0007	-0.0004	0.1063	0.0232	-0.1129	-0.1111	-0.1169	-0.0965	-0.0616	-0.0371
	Nure	NO	NO	NO	NO	-0.1403	-0.1604	-0.1772	-0.1560	-0.1262	-0.0878
	Arda	NO	NO	NO	NO	-0.1414	-0.1501	-0.1499	-0.1255	-0.0906	-0.0707
	Taro	NO	NO	NO	NO	-0.1902	-0.2031	-0.2146	-0.1989	-0.1650	-0.1355
	Parma	NO	NO	NO	NO	-0.1970	-0.2099	-0.2140	-0.1731	-0.1374	-0.1138
	Enza	NO	NO	NO	NO	-0.1572	-0.1635	-0.1571	-0.1164	-0.0910	-0.0701
	Secchia	NO	NO	NO	NO	-0.2469	-0.2539	-0.2348	-0.1938	-0.1665	-0.1540
	Panaro	NO	NO	NO	NO	-0.2618	***-0.2735***	-0.2600	-0.2176	-0.1893	-0.1739

Table 3. Pearson coefficient values between the logarithm of specific turbidity in the Po River at Piacenza and Pontelagoscuro and water discharge in the tributaries. The highlighted values are the highest for each station respect to an Alpine and Apennine tributary.

In Table 4, the absolute values reach a maximum of around 0.3, slightly higher than previous cases. The two highest absolute Pearson coefficient values for the Piacenza station are associated with the Tanaro for Alpine rivers and the Scrivia for the Apennine rivers. Conversely, for the Pontelagoscuro station, the highest absolute values are observed for the Oglio and Secchia rivers compared to both the Alpine and Apennine tributaries.

		PIACENZA				PONTELAGOSCURO					
		t	*t+1*	*t+2*	*t+3*	*t*	*t+1*	*t+2*	*t+3*	*t+4*	*t+5*
ALPS	*Stura*	-0.0345	-0.0258	-0.0213	0.0020	-0.1458	-0.1640	-0.1752	-0.1540	-0.1213	-0.0825
	Malone	-0.0981	-0.1006	-0.1462	-0.0797	-0.1913	-0.2130	-0.2213	-0.1952	-0.1461	-0.0940
	Orco	-0.0173	-0.0071	0.0328	0.0171	-0.1266	-0.1457	-0.1592	-0.1417	-0.1128	-0.0857
	Dora B.	0.0489	0.0595	0.0986	0.0704	-0.0339	-0.0541	-0.0773	-0.0630	-0.0380	-0.0263
	Sesia	-0.0955	-0.0860	0.0733	-0.0284	-0.2181	-0.2559	-0.2863	-0.2429	-0.1868	-0.1462
	Tanaro	-0.1555	***-0.1614***	0.0077	-0.1183	-0.2521	-0.2711	-0.2876	-0.2547	-0.1930	-0.1468
	Ticino	-0.0537	-0.0497	0.1333	-0.0528	0.0113	0.0175	0.0295	0.0500	0.0762	0.0664
	Lambro	-0.0530	-0.0682	0.0820	-0.0626	-0.0972	-0.1201	-0.1841	-0.1562	-0.1080	-0.0642
	Adda	NO	NO	NO	NO	-0.2305	-0.2511	-0.2373	-0.2035	-0.1627	-0.1408
	Oglio	NO	NO	NO	NO	-0.2737	***-0.3298***	-0.3081	-0.2784	-0.1624	-0.1667
	Mincio	NO	NO	NO	NO	-0.0783	-0.0620	-0.0443	-0.0295	-0.0350	-0.0221
APPENNINES	*Scrivia*	-0.1152	***-0.1277***	0.0796	-0.0627	-0.2001	-0.2315	-0.2713	-0.2390	-0.1840	-0.1434
	Tidone	-0.0885	-0.0971	0.1121	-0.0691	-0.1331	-0.1595	-0.1615	-0.1420	-0.0959	-0.0668
	Trebbia	-0.0158	-0.0306	0.0833	0.0166	-0.1505	-0.1787	-0.2102	-0.1759	-0.1275	-0.0842
	Nure	NO	NO	NO	NO	-0.1439	-0.1890	-0.2353	-0.2119	-0.1748	-0.1128
	Arda	NO	NO	NO	NO	-0.2060	-0.2333	-0.2438	-0.1914	-0.1431	-0.1167
	Taro	NO	NO	NO	NO	-0.2093	-0.2514	-0.2955	-0.2695	-0.2250	-0.1703
	Parma	NO	NO	NO	NO	-0.2612	-0.2985	-0.3125	-0.2514	-0.1909	-0.1460
	Enza	NO	NO	NO	NO	-0.1607	-0.1827	-0.1809	-0.1305	-0.1031	-0.0762
	Secchia	NO	NO	NO	NO	-0.3022	***-0.3251***	-0.2953	-0.2388	-0.1954	-0.1691
	Panaro	NO	NO	NO	NO	-0.2840	-0.3239	-0.3069	-0.2447	-0.1946	-0.1658

Table 4. Pearson coefficient values between the logarithm of specific turbidity in the Po River at Piacenza and Pontelagoscuro and the logarithm of water discharge in the tributaries. The highlighted values are the highest for each station respect to an Alpine and Apennine tributary.

The correlations associated with the highlighted values in the three tables (Table 2, Table 3 and Table 4) were further analyzed graphically using MATLAB. The following graphs (Figure 15, Figure 16 and Figure 17) illustrate the trend of specific turbidity against the duration curve, with the color of the points indicating the water discharge in the Po River for the respective station under consideration.

In Figure 15, the relationship between the duration curve and the specific turbidity for the values highlighted in Table 2 has been examined. It is noteworthy that the discharges in the Po River at Piacenza are generally lower, with maxima just exceeding 4000 m^3/s. This can be attributed to the fact that the Po River in Piacenza has not yet reached its maximum water capacity, which is typically achieved at Pontelagoscuro, with values of discharge maxima around 8000 m^3/s. This discrepancy in values arises from the different drainage area between the stations of Piacenza and Pontelagoscuro. In Piacenza, the drainage area measures 42,030 km^2, whereas in Pontelagoscuro, it is just under twice as large, approximately 70,091 km^2.

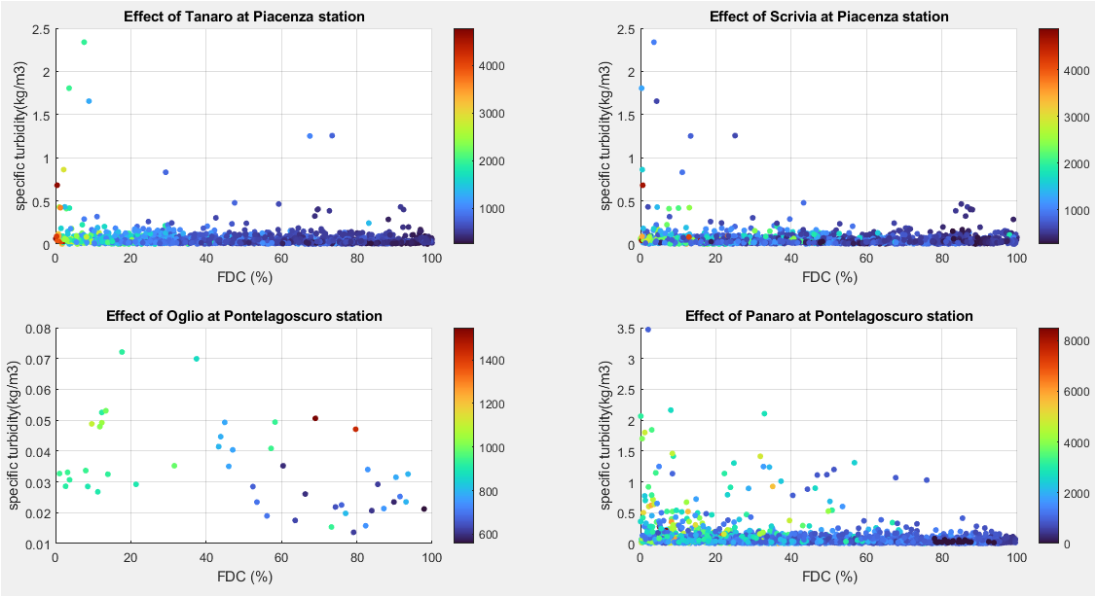

Figure 15. Specific turbidity (kg/m^3) as a function of the duration curve, where the color of the points indicates the discharge in the Po River at Piacenza or Pontelagoscuro. This graph illustrates the highest Pearson coefficient values for the Piacenza station with respect to Apennine and Alpine tributaries, as well as the highest Pearson coefficient values for the Pontelagoscuro station with respect to Apennine and Alpine tributaries.

In the graph pertaining to the Oglio River (Figure 15), the scale regarding the discharges in the Po River is limited to values approximately around 1500 m^3/s, owing to the significant lack of data in the database concerning the discharges of the Oglio River. Consequently, measures of specific turbidity in the Po River, duration curves values for

the Oglio River, and water discharge in the Po River are available at the same time only for very few events. In all four representations, a horizontal gradient can be observed, wherein the discharges in the Po River increases with the rise in water discharges in the tributary.

In Figure 16 and Figure 17, the same processing as in Figure 15 has been conducted, with the exception that the cases highlighted in Table 3 and Table 4 have been considered. In Figure 16, the specific turbidity is represented logarithmically, while in Figure 17, both the specific turbidity and the capacity are logarithmic. In this series of representations, a horizontal gradient can often be observed, indicating a hydraulic connection between rivers. However, there isn't a distribution that permit the correlation of specific turbidity with duration curves, as suggested by the values of the Pearson coefficient, which tend towards 0.

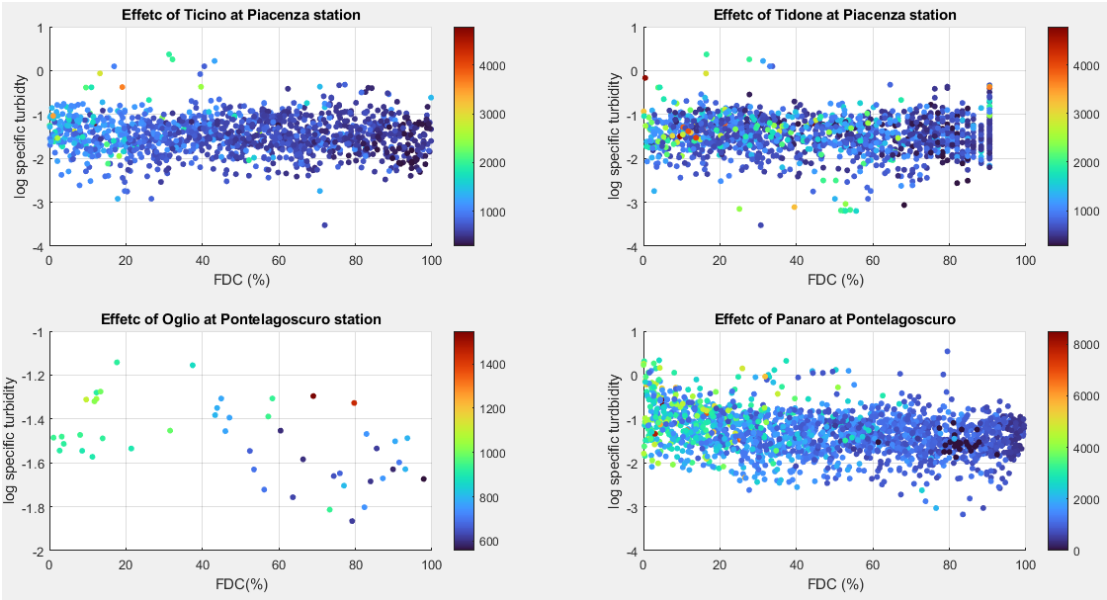

Figure 16. The logarithm of the specific turbidity as a function of the duration curve, where the color of the points indicates the discharge in the Po River at Piacenza or Pontelagoscuro. This graph represents the highest Pearson coefficient values for the Piacenza station with respect to Apennine and Alpine tributaries, as well as the highest Pearson coefficient values for the Pontelagoscuro station with respect to Apennine and Alpine tributaries.

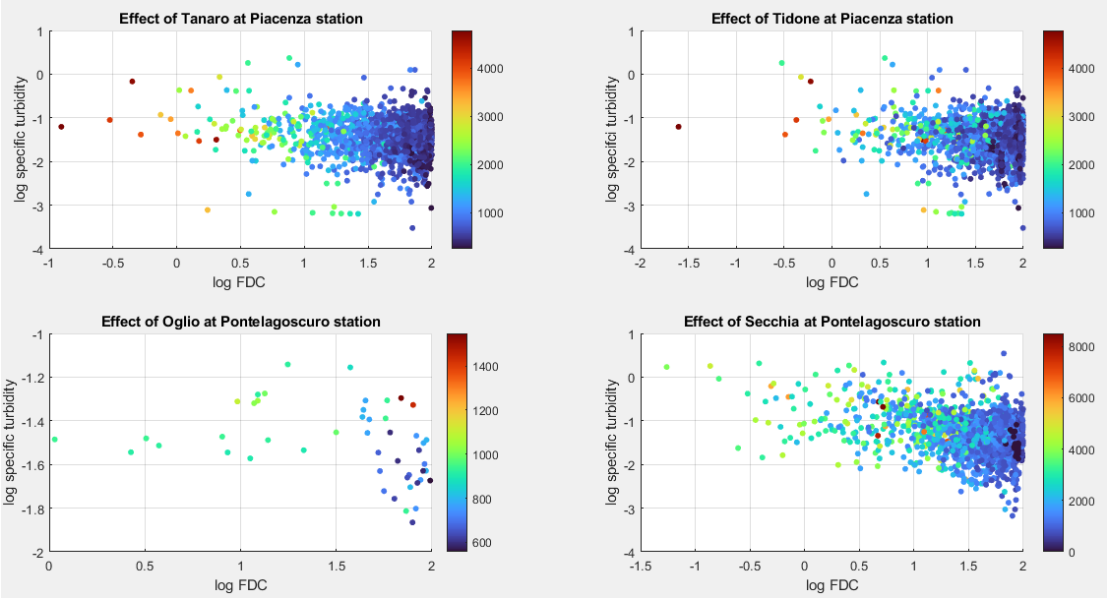

Figure 17. The logarithm of the specific turbidity as a function of the logarithm of the duration curve, where the color of the points indicates the discharge in the Po River at Piacenza or Pontelagoscuro. This graph represents the highest Pearson coefficient values for the Piacenza station with respect to Apennine and Alpine tributaries, as well as the highest Pearson coefficient values for the Pontelagoscuro station with respect to Apennine and Alpine tributaries.

To enhance the depth of the analysis, the methodology used for representing Figure 15, Figure 16 and Figure 17 was also applied to Figure 18, Figure 19 and Figure 20, with the distinction that the third variable considered, which determines the coloration of the points within the graph, is based on *AAFI* values. In Figure 18, Figure 19 and Figure 20, it is evident that the *AAFI* values are notably higher at the Piacenza station. This is primarily due to the fact that most of the Alpine tributaries are situated upstream of this station, while 7 out of 10 tributaries from the Apennines are located downstream of it. At Pontelagoscuro, all the tributaries contribute to the *AAFI* values.

In Figure 18, it is evident that for the Alpine tributaries (in this case Tanaro and Oglio), a well-defined horizontal gradient or a recognizable distribution of points is not apparent. However, for the Apennine tributaries (in this case Scrivia and Panaro), a horizontal gradient is observed, where the *AAFI* value increases as the water discharge in the tributary decreases. This phenomenon can be readily explained by the equation of the *AAFI* (1).

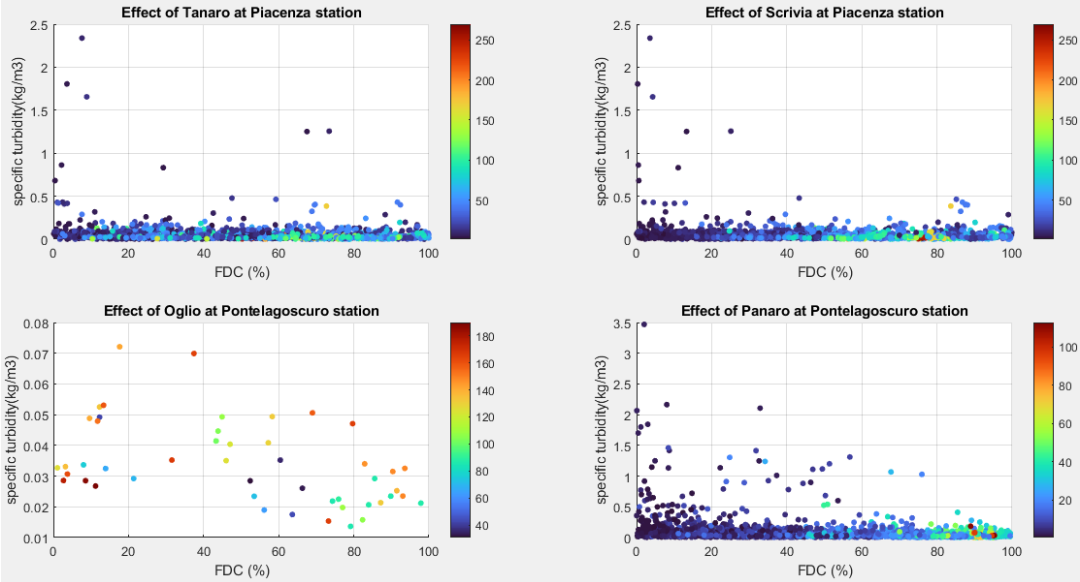

Figure 18 . Specific turbidity (kg/m³) as a function of the duration curve, where the color of the points indicates the value of AAFI. This graph represents the highest Pearson coefficient values for the Piacenza station with respect to Apennine and Alpine tributaries, as well as the highest Pearson coefficient values for the Pontelagoscuro station with respect to Apennine and Alpine tributaries.

In the subsequent representations (Figure 19 and Figure 20,) the same observations as those made in Figure 18 hold true. Specifically, the well-defined horizontal gradient is evident only for the Apennine tributaries (Tidone and Panaro in Figure 19 and Tidone and Secchia in Figure 20), where the AAFI increases as the discharge of the tributary decreases.

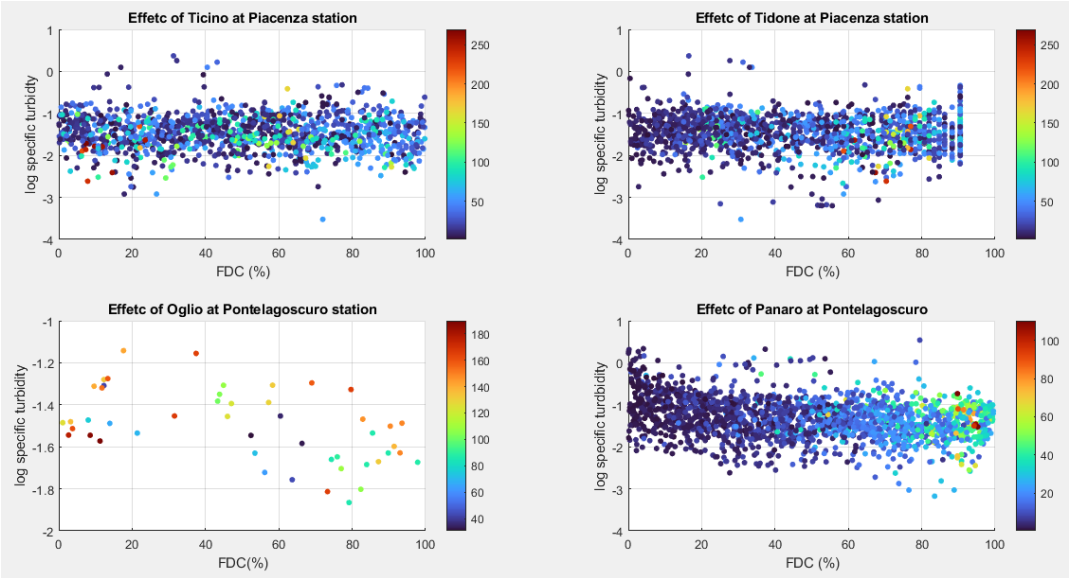

Figure 19. The logarithm of the specific turbidity, as a function of the duration curve, where the color of the points indicates the value of AAFI. This graph represents the highest Pearson coefficient values for the Piacenza station with respect to Apennine and Alpine tributaries, as well as the highest Pearson coefficient values for the Pontelagoscuro station with respect to Apennine and Alpine tributaries.

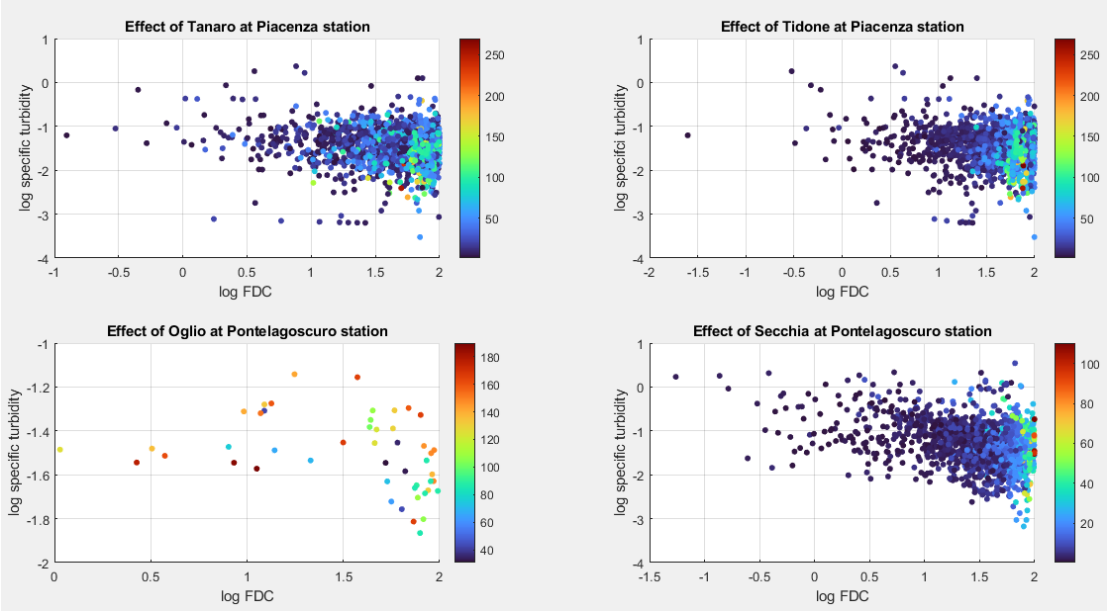

Figure 20. The logarithm of the specific turbidity as a function of the logarithm of the duration curve, where the color of the points indicates the value of AAFI. This graph represents the highest Pearson coefficient values for the Piacenza station with respect to Apennine and Alpine tributaries, as well as the highest Pearson coefficient values for the Pontelagoscuro station with respect to Apennine and Alpine tributaries."

4.2 Analysis of time patterns and seasonality in the SST

The second part of the analysis focused on identifying the controlling factors of suspended sediment transport, exploring seasonality and temporal tendencies within the 2009-2019 study period. This investigation focused exclusively on Pontelagoscuro, as it serves as the primary measuring station for basin closure. Thus, Pontelagoscuro is deemed representative of the overall behavior of the entire basin.

In Figure 21 three distinct years with varying trends were identified. One year exhibited significantly higher water discharges and lower specific turbidity values (2014), another year showed a narrower range of water discharges but higher turbidity values (2016), while a third year (2010) demonstrated intermediate behavior.

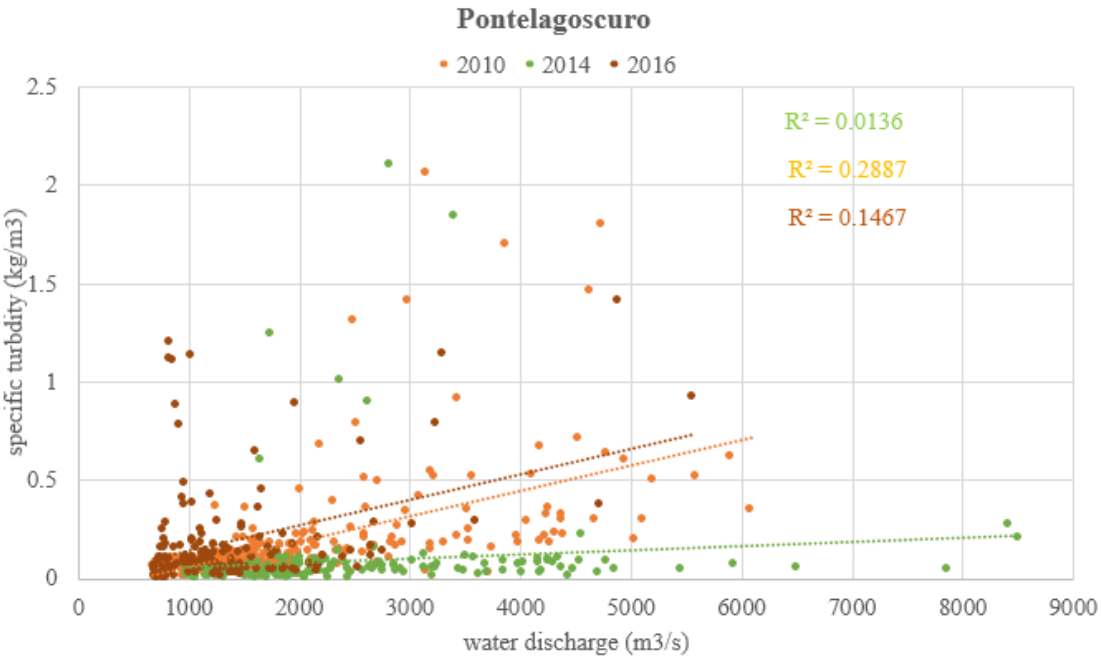

Figure 21. Specific turbidity (kg/m³) as a function of water discharge (m³/s) for the Pontelagoscuro station, with three years exhibiting distinct characteristics highlighted (2010, 2014, and 2016).

Further analysis of events with specific turbidity values exceeding 0.4 revealed a monthly distribution, with a notable concentration in the autumn period, except for June in 2010, which also experienced elevated turbidity values (Table 5 and Figure 22).

Table 5. Monthly distribution of specific turbidity values above 0.4 kg/m³, for the years 2010, 2014 and 2016.

	2010	***2014***	***2016***
January	0	0	0
February	2	0	2
March	1	0	3
April	1	0	0
May	2	0	0
June	5	0	0
July	0	0	0
August	0	0	0
September	0	0	1
October	2	5	0
November	5	1	11
December	6	0	0

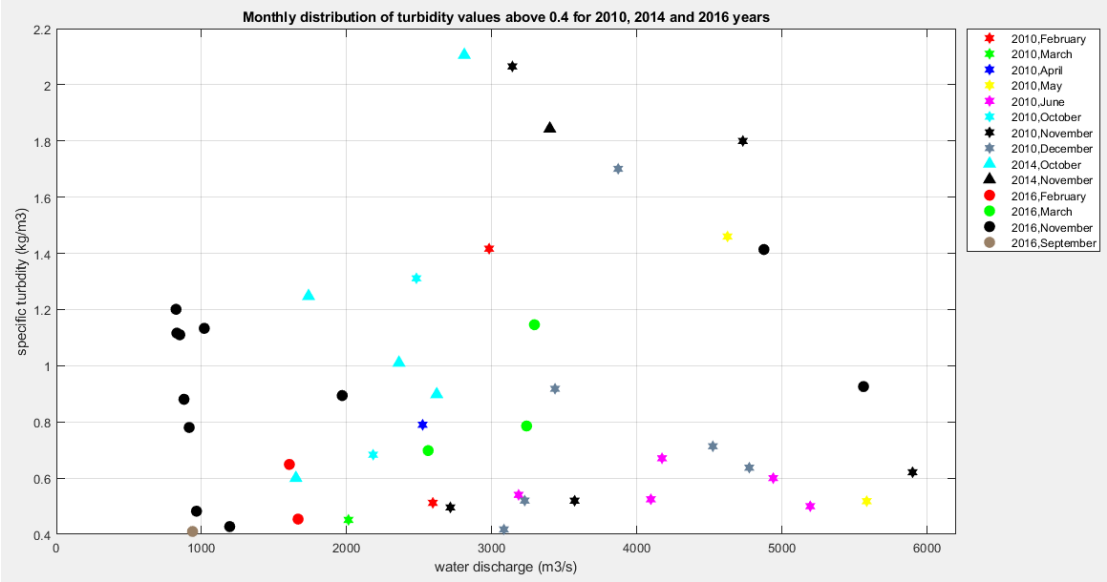

Figure 22. Specific turbidity (kg/m³) as a function of water discharge (m³/s) for specific turbidity values above 0.4 kg/m³, for the years 2010, 2014, and 2016. The same years are represented by the same symbols, and the same months are illustrated with the same color.

These findings prompted a time series analysis of specific turbidity and water discharge at Pontelagoscuro (Figure 23). Within the time series, potential correspondences between discharge peaks and turbidity peaks were investigated, alongside an examination of trends in suspended sediment transport behavior.

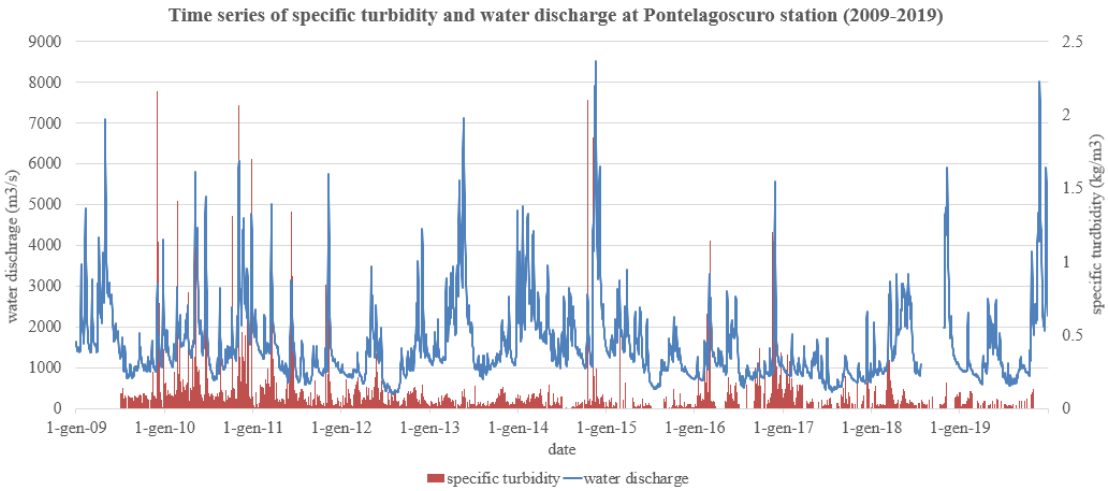

Figure 23. Time series of specific turbidity and mean daily water discharge of the Po River at Pontelagoscuro station (2009-2019).

The final analysis employed a series of Box Plots. The first two Box Plots (Figure 24 and Figure 25) compared the entire dataset of specific turbidity and water discharge data with their respective months of observation.

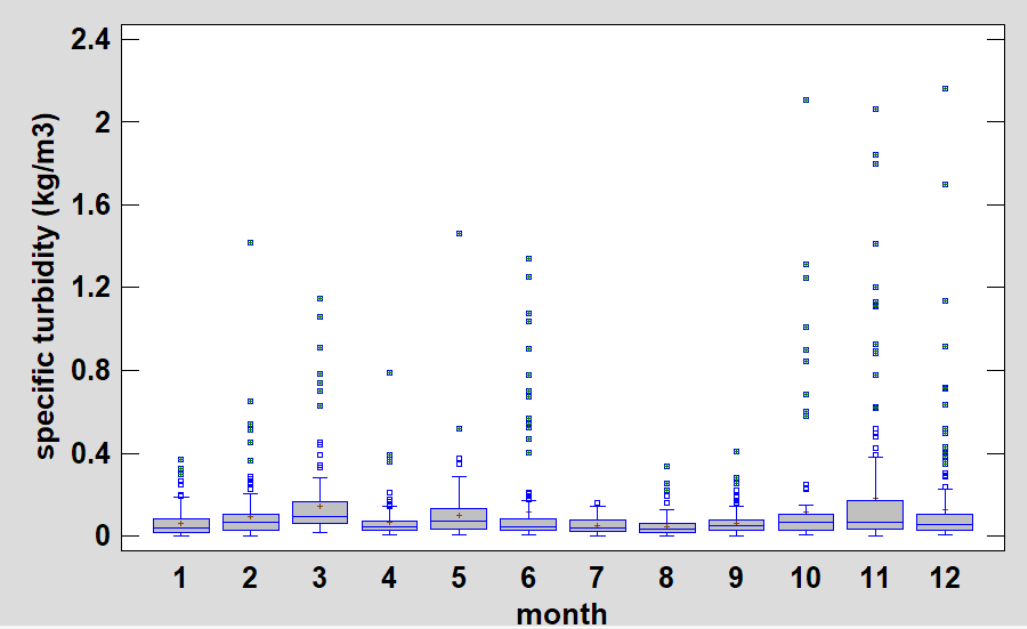

Figure 24. Box plot illustrating specific turbidity (kg/m³) distribution across months for all values in the time series. The numbers on the x-axis indicate the month of the year.

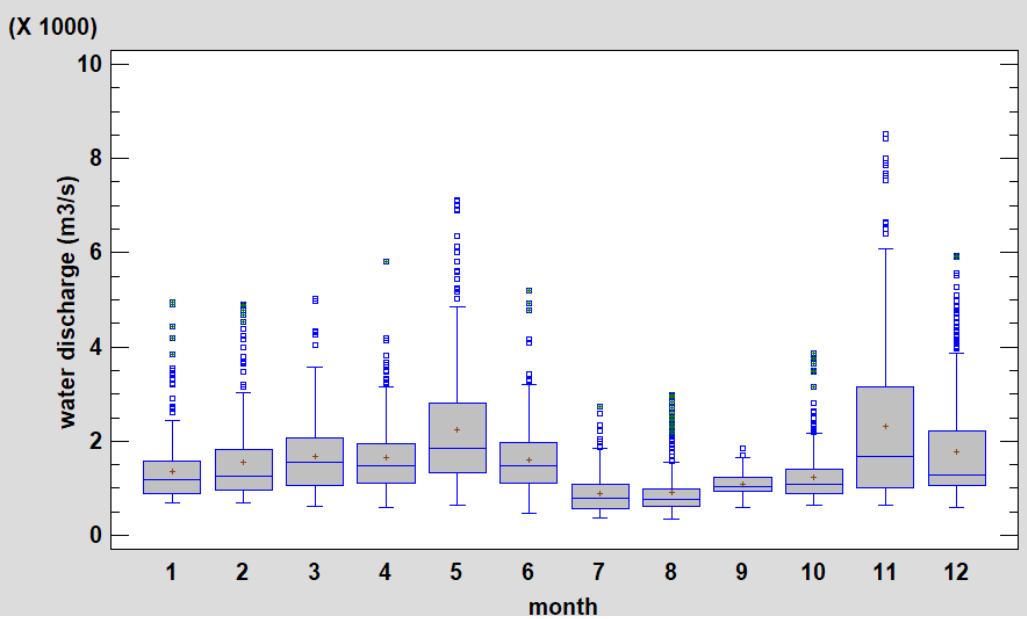

Figure 25. Box plot illustrating water discharge (m³/s) distribution across months for all values in the time series. The numbers on the x-axis indicate the month of the year.

For Figure 24, the highest range of turbidity values were recorded in November, March and June, however the median is higher in March, May and October. In Figure 25, relating to discharges, the highest values are reached in November and May, which is also reflected by the median values (Table 6). The last two Box Plots (Figure 26 and Figure 27) compared specific turbidity or water discharge data with their respective months of observation, focusing exclusively on values above the 90th percentile. For

water discharges, this threshold corresponded to 2739.4 m^3/s, while for specific turbidity to 0.177 kg/m^3. Observing these charts, October emerges as the month with the highest specific turbidity values (Figure 26), followed by November, December, and June. In contrast, for discharges (Figure 27), November experiences the highest peaks, followed by December and June. Although October does not reach similarly high peaks, it maintains a median higher than the majority of the other months.

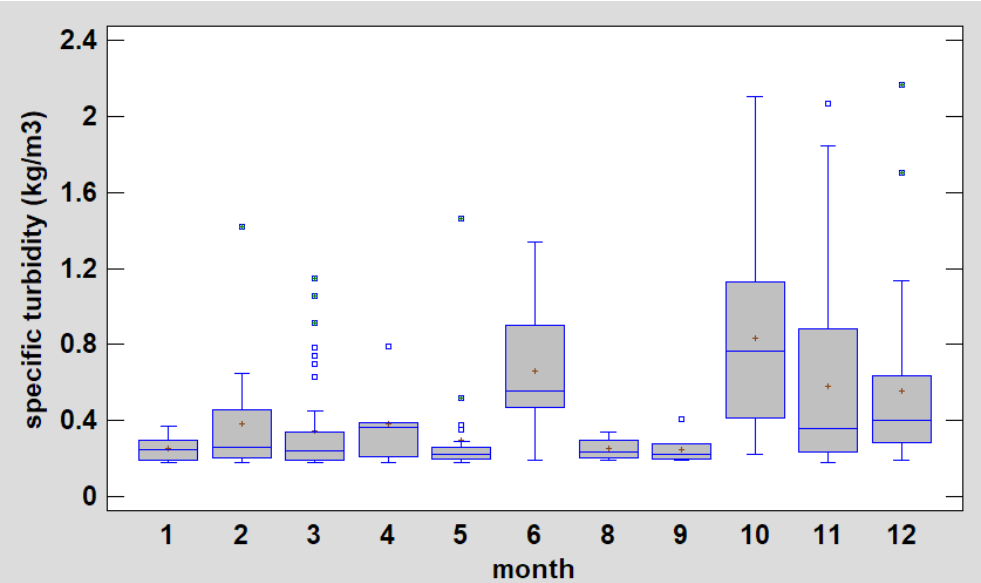

Figure 26. Box plot illustrating specific turbidity (kg/m^3) distribution across months for values above the 90th percentile of specific turbidity. The numbers on the x-axis represent the month of the year.

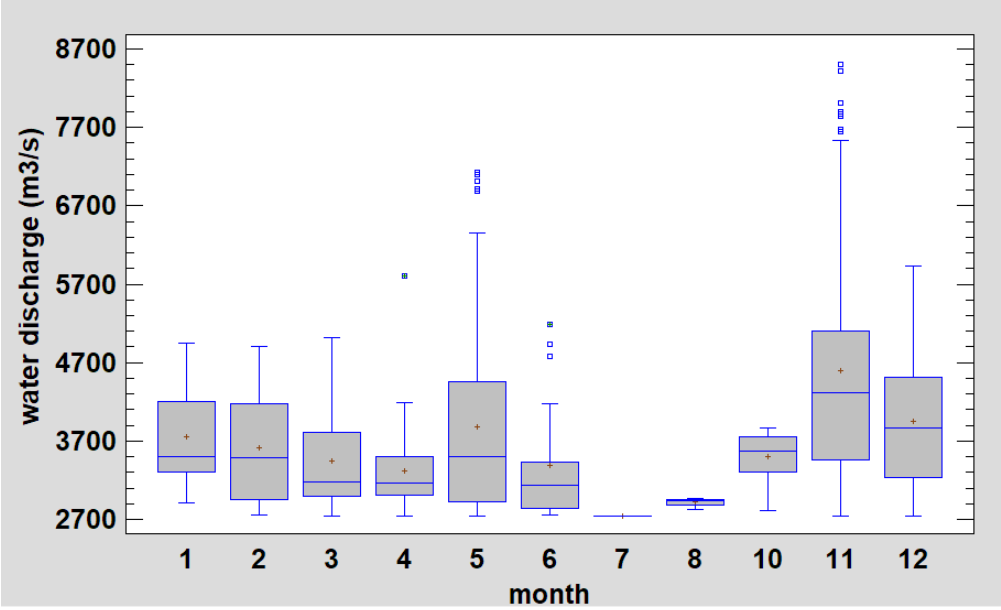

Figure 27. Box plot illustrating water discharge (m^3/s) distribution across months for values above the 90th percentile of specific turbidity. The numbers on the x-axis represent the month of the year.

As a final step, a summary table (Table 6) was created based on the information already presented in the box plots. This table displays the median and mean values for the 90th percentiles of water discharge and turbidity, as well as the mean and median values for the entire dataset. In the last part of this table, the ratio between the mean or median of specific turbidity and the discharge for values above the 90th percentile was calculated, providing insights into the months with higher concentrations of suspended sediments in the water column. The same analysis was conducted for mean and median values for the entire discharges and specific turbidity dataset.

		January	February	March	April	May	June	July	August	September	October	November	December
water discharge 90th percentile	**median**	3499.00	3483.00	3175.50	3158.26	3506.00	3129.76	2742.40	2942.15	\	3575.63	4319.61	3870.00
(m3/s)	**mean**	3759.87	3610.58	3439.54	3318.39	3879.17	3382.07	2742.40	2921.33	\	3494.75	4596.23	3955.53
time series water discharge	**median**	1194.00	1246.61	1549.55	1485.60	1847.24	1485.81	795.00	746.35	1018.94	1038.07	1673.08	1286.24
(m3/s)	**mean**	1358.02	1544.47	1681.78	1652.96	2245.18	1600.53	875.36	835.88	992.58	1130.33	2306.12	1761.28
spefici turdbidity 90th percentile	**median**	0.247700	0.257000	0.239467	0.364483	0.222177	0.553017	\	0.236993	0.219538	0.762750	0.356133	0.400633
(kg/m3)	**mean**	0.250959	0.380030	0.346110	0.382503	0.296444	0.661972	\	0.251563	0.248625	0.831804	0.578169	0.556974
time series specific turbidity	**median**	0.035586	0.063633	0.095000	0.046567	0.070400	0.045567	0.040158	0.031900	0.047553	0.066467	0.063650	0.054352
(kg/m3)	**mean**	0.060096	0.094274	0.144575	0.067785	0.100590	0.113674	0.051866	0.046283	0.059750	0.114876	0.183285	0.126987
ratio between median of the 90th percentile		0.000071	0.000074	0.000075	0.000115	0.000063	0.000177	\	0.000081	\	0.000213	0.000082	0.000104
ratio between mean of the 90th percentile		0.000067	0.000105	0.000101	0.000115	0.000076	0.000196	\	0.000086	\	0.000238	0.000126	0.000141
total ratio between the median of the time series		0.000030	0.000051	0.000061	0.000031	0.000038	0.000031	0.000051	0.000043	0.000047	0.000064	0.000038	0.000042
total ratio between the mean of the time series		0.000044	0.000061	0.000086	0.000041	0.000045	0.000071	0.000059	0.000055	0.000060	0.000102	0.000079	0.000072

Table 6. Summary table of results obtained with Box Plots. The first two rows represent the mean and median for discharges values above the 90th percentile and for the all the discharge values in the complete time series. The subsequent two rows depict the mean and median for specific turbidity values above the 90th percentile and for all the specific turbidity values in the complete time series. The last four lines indicate the ratio between the median or mean specific turbidity and water discharge above the 90th percentile, followed by the same comparison for the entire time series.

5 Discussion

5.1 Contribution of Alpine and Apennine tributaries to the suspended sediment transport in the Po River

The graphs where the specific turbidity is expressed as a function of the water discharge for the four stations (Figure 8 and Figure 9) attempts to delineate three distinct zones representing the tributary contributions of the Alpine tributaries, the Apennines, and a mixture of the two. In the analysis conducted using the *AAFI*, as depicted in the Figure 11 and Figure 12, a variety of index values can be observed. For Piacenza, levels reach up to 140, whereas for Pontelagoscuro, values decrease to as low as 45. Values below one would suggest a stronger water contribution of the Appenines rivers, while values exceeding one would indicate a stronger Alpin water contribution. These values confrim the assertion made by Del Longo (2018) and Syvitski & Kettner (2007). that the water supply from the Apennine region is significantly lower that the one from the Alps. Regarding specific turbidity in Figure 11 and Figure 12, we observe a maximum of 0.41 kg/m^3 at Piacenza, while Pontelagoscuro records a peak of 1.31 kg/m^3. This disparity is due to the predominantly Alpine river contribution at Piacenza, resulting in a higher *AAFI* and lower turbidity. In Pontelagoscuro, however, with contributions from all twenty-one tributaries, turbidity increases, inversely affecting the *AAFI*. These values of *AAFI* consistently exceeding 1, often by a significant margin, providing additional evidence to support the notion of Del Longo (2018) and Syvitski & Kettner (2007) that the Apennines water supply to the Po River is significantly limited.

Upon initial analysis on the graph related to Pontelagoscuro station (Figure 12), it appears that a decrease in the *AAFI* corresponds to either a reduction in water discharges from Alpine tributaries or an increase in discharges from Apennine tributaries, leading to increased specific turbidity.

To provide a more rigorous assessment of this trend, the Pearson coefficient was employed (Table 2, Table 3 and Table 4). While generally exhibiting relatively low values, with maximum peaks typically around 0.2, except for the Oglio River where the scarcity of discharge data (missing data exceeding 70%) from 2009-2019 likely impacts the analysis. Pearson coefficients trending towards zero clearly indicate a lack

of statistical correlation between the two variables (Nettleton et al, 2014). To support these findings, the highest Pearson coefficient values calculated for stations in Piacenza and Pontelagoscuro were compared with those of the Alpine and Apennine tributaries (Figure 15, Figure 16 and Figure 17). Across all three analyses, no discernible trend is apparent. However, a horizontal gradient observed in this instance merely suggests a water-based correlation between the tributaries and the Po, wherein an increase in tributaries water discharge (especially in the Panaro River) corresponds to increased water discharge in the Po.

The expectation that was not fulfilled was the anticipation of observing a downward trend, particularly related to Apennines tributaries, wherein high discharges in the tributaries would correspond to moderate/high water discharges in the Po River and elevated turbidity levels. It was expected that a decrease in water discharge in the tributaries would also result in decreased turbidity values. However, this anticipated relationship did not materialize. This observation underscores the limited correlation between the tributaries and the *SST* in the Po River.

Regarding the same analysis but using the *AAFI* diagram's point coloration index (Figure 18, Figure 19 and Figure 20), it can be noted that no significant relationships are evident. Only a horizontal gradient is observed, where the index increases with decreased water discharge. This phenomenon occurs because as water discharge in a given Apennine tributary decreases, the *AAFI* ratio consequently increases.

The analyzed data, spanning from 2009 to 2019, do not reveal a significant influence of the Apennine tributaries on the turbidity of the Po River. Although the turbidity values and the sediment transport of the Apennine rivers are higher than those of the Alps (De Longo, 2018; Van Rompaey et al., 2005; Raiteri, 1994), the Alpine rivers boast considerably higher water discharges, as evidenced by the *AAFI* values obtained. Consequently, the Apennine tributaries lack the capacity to significantly influence the turbidity values of the Po River because of a dilution process. To explain these results, we can speculate that the absolute suspended sediment transport of the Apennine tributaries is not greater when compared to the Alpine rivers due to their considerably smaller water discharge, a fact highlighted by the *AAFI* values consistently exceeding 1. Furthermore, the specific turbidity values at Pontelagoscuro, commonly observed in

the Po River, predominantly fall below 0.5 kg/m^3 (Figure 9), a value more closely resembling that of the Alpine rivers rather than the Apennines (Raiteri, 1994).

5.2 Analysis of time patterns and seasonality in the SST

Figure 21 was used to examine three years exhibiting distinct behaviors in suspended sediment transport and discharge of the Po River. Subsequently, we delved into a detailed study of the timing of various events depicted in Figure 21 within each month. It was hypothesized that suspended sediments were more prone to increase in the river channel with the first modest discharges in autumn after a period of low discharges and precipitation like summer. The hypothesis made was that with the first rains, medium to light precipitation events would lead to an increase in surface runoff and consequently on the suspended sediment transport, as observed for other Mediterranean basins (Rovira & Batalla, 2006; Millares et al, 2020; Pagano et al, 2019).

To substantiate this hypothesis, we proceeded with data analysis, particularly focusing on turbidity values. The events with the highest turbidity values, compared among the three years under consideration (Table 5), were primarily concentrated in the autumn period, coinciding with the season of highest precipitation. An exception was noted in 2010, where a significant number of events occurred in June.

Upon analyzing the time series data (Figure 23), certain years exhibited similarities in terms of peak turbidity values. Specifically, 2016 and 2017 resembled 2010 and 2011, characterized by considerable peak turbidity values exceeding 0.5 kg/m³, while 2013, 2014, 2018, and 2019 demonstrated substantially lower specific turbidity values with almost no peaks. Initial analysis indicates that turbidity peaks do not necessarily correspond to specific hydrological signals (Syvitski & Kettner, 2007); however, many coincide with the end of periods of relatively low water discharge.

To delve deeper into this phenomenon, we generated two pairs of box plots (Figure 24, Figure 25, Figure 26 and Figure 27). The box plots for 90th percentile values (Figure 26 and Figure 27) revealed that the highest turbidity values occurred in October, following the summer period characterized by low sediment transport and water discharges. This observation supports the theory that a subsequent decrease in river discharge, induced by periods of low precipitation such as summer, would decrease the

connectivity between the catchment and the main stem of the Po River. This process is attributed to the reduced surface runoff within the catchment. Subsequently, these sediments will be flushed out by the first rains with average or slightly higher water discharge values, resulting in peak specific turbidity. However, a turbidity peak observed in June presents a more complex interpretation, likely attributed to the melting of the last layers of snow (Syvitski & Kettner, 2007; Cattaneo et al, 2003) in high-altitude areas, which carry substantial sediment loads despite limited water intake compared to the major snowmelt events in May.

Considering the entire time series (Figure 24 and Figure 25), a correlation emerges between months with high water discharge values and those with high specific turbidity values, notably June and November. However, even in these cases, November demonstrates a turbidity peak following a period of low water discharge in late summer and early autumn. These findings are reinforced by the relationships highlighted in the Table 6, where the ratio above the 90th percentile and for the entire time series are highest in October, followed by December.

The behavior of specific turbidity in the Po River appears to have a sort of seasonality and to be influenced by summer dry periods, which reduce surface hillslope runoff. This reduction is followed by increased sediment transport during the first rain period and the average water discharges of October, like for other Mediterranean river basins as proved by Rovira & Batalla., 2006, Millares et al., 2020 and Pagano et al, 2019.

6 Conclusions

The study of suspended sediment transport has long been a complex subject due to its significant temporal and spatial variability (De Girolamo et al., 2015; Vercruysse et al., 2017), as well as the multitude of factors influencing this phenomenon. In this study, our focus lies primarily on two aspects: the contribution of sediment from Alpine or Apennine tributaries to the suspended load in the Po River between 2009 and 2019, and the examination of seasonal variations.

The initial analysis concerning river tributaries was grounded in the concept that Apennine rivers exhibit higher turbidity (Raiteri, 1994) and lower water discharges compared to Alpine rivers (De Longo, 2018; Van Rompaey et al., 2005). However, it was not possible to assess the specific contribution of the Apennine tributaries to the turbidity of the Po River during individual flood events between 2009 and 2019. Instead, it emphasized the significance of the Alpine tributaries' water supply to the Po River. Based on results of this study, it can be concluded that the Apennine tributaries have a relatively minor impact on the turbidity of the Po River due to a dilution process as a result of substantially higher discharge of Alpine rivers, as evidenced by the *AAFI* values that were obtained. In addition, the specific turbidity values commonly observed at Pontelagoscuro in the Po River, mostly below 0.5 kg/m^3, bear a closer resemblance to those of the Alpine rivers rather than the Apennines (Raiteri, 1994).

Conversely, the investigation into seasonality revealed more noteworthy findings. It has been observed that *SST* exhibits a certain seasonality, notably with peaks occurring in October and November, as well as a peak in June. This behavior resembles the behavior of others Mediterranean basins (Rovira & Batalla, 2006, Millares et al., 2020 and Pagano et al, 2019). An observable increase in suspended sediment transport during the autumn period was noted, particularly following the low transport and water discharge of summer. With the onset of the first rains in October, there was a marked rise in suspended load, which could be due to a significant rise in the surface run-off within the catchment, which consequently leads to an increase in the suspended sediments in the Po main channel. High levels of suspended sediments were also observed in June, likely attributed to the melting of snow (Syvitski & Kettner, 2007)

from the highest peaks, rich in sediment but with limited water supply. This hypothesis warrants further exploration in subsequent studies.

However, this work underscores the inherent randomness of suspended load in the Po River and its intricate interpretation. Several factors contribute to this complexity, including the quality of measured data on suspended sediment transport, which in this case was focused on the finest sediment (wash load) and only on the first layer of the water column. The wash load represents only a fraction of the total suspended sediments in the water column, implying that the data used in this study are not fully representative of the total suspended load in the Po River. Additionally, sampling solely from the upper part of the water column further limits the scope of these data, as they do not provide a comprehensive representation of the entire water column. Moreover, the lack of adherence to rigorous sampling standards has posed challenges in obtaining conclusive results, particularly in the initial phase of this research concerning the contribution of the Alpine/Apennine tributaries to the turbidity of the Po River. Furthermore, the study only accounts for some of the primary factors influencing suspended sediment transport, suggesting that more comprehensive analyses may yield more conclusive results.

7 References

- Autorità di Bacino del Fiume Po: Il recupero morfologico ed ambientale del fiume Po, 2008.
- Babìnski Z, The relationship between suspended and bed load transport in river channels. Sediment Budgets 1 (Proceedings of symposium S1 held during the Seventh IAHS Scientific Assembly at Foz do Iguaçu, Brazil, April 2005). IAHS Publ. 291, 2005
- Bagnold R. A., 1973, The nature of saltation and of 'bed-load' transport in water, Proc. R. Soc. Lond. A332473–504. http://doi.org/10.1098/rspa.1973.0038
- Bai J, Fang H, Stoesser T. 2013. Transport and deposition of fine sediment in open channels with different aspect ratios. Earth Surface Processes and Landforms 38: 591-600
- Bever Aaron J, Harris Courtney K., Sherwood Christopher R., Signell Richard P., Deposition and flux of sediment from the Po River, Italy: An idealized and wintertime numerical modeling study, Marine Geology, Volume 260, Issues 1–4, 2009, Pages 69-80, ISSN 0025-3227, https://doi.org/10.1016/j.margeo.2009.01.007.
- Billi P., Spalevic V., Suspended sediment yield in Italian rivers, CATENA, Volume 212, 2022, 106119, ISSN 0341-8162, https://doi.org/10.1016/j.catena.2022.106119.
- Brenna A., Bizzi S., Surian N., How multiple anthropic pressures may lead to unplanned channel patterns: Insights from the evolutionary trajectory of the Po River (Italy), CATENA, Volume 234, 2024, 107598, ISSN 0341-8162, https://doi.org/10.1016/j.catena.2023.107598.
- Brenna, A., Bizzi, S. & Surian, N. (2022) A width-based approach to estimating historical changes in coarse sediment fluxes at river reach and network scales. Earth Surface Processes and Landforms, 1–20. Available from: https://doi.org/10.1002/esp.5395
- Bridge, J., 2003. Rivers and Floodplains: Forms, Processes, and Sedimentary Record. Blackwell Science, Oxford.

- Burgan H. I., Aksoy H., Daily flow duration curve model for ungauged intermittent subbasins of gauged rivers, Journal of Hydrology, Volume 604, 2022, 127249, ISSN 0022-1694, https://doi.org/10.1016/j.jhydrol.2021.127249.
- Cattaneo A, Correggiari A, Langone L et al (2003) The late-Holocene Gargano subaqueous delta, Adriatic shelf: sediment pathways and supply fluctuations. Mar Geol 193:61–91
- Church M. (2006). Bed material transport and the morphology of alluvial river channels. Annu. Rev. Earth Planet. Sci., 34, 325-354.
- De Girolamo A.M., Pappagallo G., Lo Porto A., Temporal variability of suspended sediment transport and rating curves in a Mediterranean river basin: The Celone (SE Italy), CATENA, Volume 128, 2015, Pages 135-143, ISSN 0341-8162, https://doi.org/10.1016/j.catena.2014.09.020.
- Del Longo M., 2018, Sediment management in channel networks: from measurements to best practices, Sediment transport monitoring and management plans in Italy, ARPAE.
- Domeneghetti A., Castellarin A., Brath A., (2011). Assessing rating-curve uncertainty and its effects on hydraulic model calibration. Hydrology and Earth System Sciences Discussions. 8. 10501-10533. 10.5194/hessd-8-10501-2011.
- Faizi N., Alvi Y., Biostatistics Manual for Health Research, Academic Press, 2023, Pages 109-126, ISBN 9780443185502, https://doi.org/10.1016/B978-0-443-18550-2.00002-5.
- Fondriest Environmental, Inc. "Sediment Transport and Deposition." Fundamentals of Environmental Measurements. 5 Dec. 2014. Web. < https://www.fondriest.com/environmental-measurements/parameters/hydrology/sediment-transport-deposition/ >.
- Garcia M. (2008). Sediment Transport and Morphodynamics. 10.1061/9780784408148.ch02.
- ISPRA, Metodologie di misura e specifiche tecniche per la raccolta e l'elaborazione dei dati idrometeorologici, Manuali e Linee Guida 60/2010, ISBN 978-88-448-0442-8.
- ISPRA, 2014, Appennini, https://www.isprambiente.gov.it/files/notizie-ispra/notizia-2014/giro-italia/appennini.pdf

- ISPRA, 2014, Alpi, https://www.isprambiente.gov.it/files/notizie-ispra/notizia-2014/giro-italia/alpi.pdf
- Khullar N. K., Transport of fines/wash load through channels–a review, Hydrology Journal, 30 (3-4) July-Dec 2007, http://re.indiaenvironmentportal.org.in/files/Hydrology%20Journal%202007..pdf
- Larsen M.C.,Gellis A.C., Glysson G.D., GrayJ.R., Horowitz A.J., Fluvial sediment in the environment: a national problem Proceedings, 2nd Joint Federal Interagency Conference, Las Vegas, NV. June 27–July 1 (2010), (15 pp.).
- Marchetti M. (2002) Environmental changes in the central Po Plain (northern Italy) due to fluvial modifications and anthropogenic activities. Geomorphology, 44(3–4), 361–373. https://doi.org/10.1016/S0169-555X(01)00183-0
- Millares A., Chikh H. A., Habi M., Morsli B., Galve J. P., Perez-Peña J. V., Martín-Rosales W., (2020) Seasonal patterns of suspended sediment load and erosion-transport assessment in a Mediterranean basin, Hydrological Sciences Journal, 65:6, 969-983, DOI: 10.1080/02626667.2020.1724294
- Milliman J. D., River Inputs*, Editor(s): John H. Steele, Encyclopedia of Ocean Sciences (Second Edition), Academic Press, 2001, Pages 754-761, ISBN 9780123744739, https://doi.org/10.1016/B978-012374473-9.00074-6
- Montanari A., (2012). Hydrology of the Po River: Looking for changing patterns in river discharge. Hydrology and Earth System Sciences. 16. 3739-3747. 10.5194/hess-16-3739-2012.
- Nelson, B.W., 1970. Hydrography, sediment dispersal, and recent historical development of the Po River delta, Italy. In: Morgan, J.P. (Ed.), Deltaic Sedimentation, Modern and Ancient. SEPM Special Publication, pp. 152–184
- Nettleton D., Chapter 6 - Selection of Variables and Factor Derivation, Editor(s): David Nettleton, Commercial Data Mining, Morgan Kaufmann, 2014, Pages 79-104, ISBN 9780124166028, https://doi.org/10.1016/B978-0-12-416602-8.00006-6
- Nones M. Dealing with sediment transport in flood risk management. Acta Geophys. 67, 677–685 (2019). https://doi.org/10.1007/s11600-019-00273-7
- Pagano S. T., Rainato R., García-Rama A., Gentile F., Lenzi M. A:, (2019) Analysis of suspended sediment dynamics at event scale: comparison

between a Mediterranean and an Alpine basin, Hydrological Sciences Journal, 64:8, 948-961, DOI: 10.1080/02626667.2019.1606428

- Pähtz T., Clark A. H., Valyrakis M., Durán O. (2020). The physics of sediment transport initiation, cessation, and entrainment across aeolian and fluvial environments. Reviews of Geophysics, 58, e2019RG000679. https://doi.org/10.1029/2019RG000679
- Panagos, P., Borrelli, P., Meusburger, K., Alewell, C., Lugato, E., Montanarella, L., 2015. Estimating the soil erosion cover-management factor at the European scale. Land Use Policy 48:38–50. http://dx.doi.org/10.1016/j.landusepol.2015.05.021.
- Parsons A. J., Cooper J., Wainwright J., (2015). What is suspended sediment?. Earth Surface Processes and Landforms. 40. 10.1002/esp.3730.
- Pitlick J., Mueller E.R., Segura C. (2012) Differences in Sediment Supply to Braided and Single-Thread River Channels: What Do the Data Tell Us? In: Church, M., Biron, P.M. & Roy, A.G. (Eds.), Gravel-Bed Rivers: Processes, Tools, Environments. Hoboken, NJ: John Wiley & Sons, pp. 502–511. https://doi.org/10.1002/9781119952497.ch35
- Ponce M. V., 1994-2024, Prof. Miguel Victor Ponce's website, https://ton.sdsu.edu/cive530_lecture_17b.html
- Raiteri E., 1994. Un'analisi del trasporto solido in sospensione nei fiumi italiani. Idrotecnica, n. 3, maggio-giugno 1995
- Rodrigues S., & Claude N., & Moatar F., (2012). Sediment Transport. 10.1002/9780470057339.vas010.pub2.
- Rovira A., Batalla R. J., Temporal distribution of suspended sediment transport in a Mediterranean basin: The Lower Tordera (NE SPAIN), Geomorphology, Volume 79, Issues 1–2, 2006, Pages 58-71, ISSN 0169-555X, https://doi.org/10.1016/j.geomorph.2005.09.016.
- Sader, M. (2017). Turbidity measurement: A simple, effective indicator of water quality change. OTT Hydromet. Retrieved from http://www. ott. com/en-us/products/download/turbidity-white-paper.
- Syvitski J.P.M., Kettner A. J., On the flux of water and sediment into the Northern Adriatic Sea, Continental Shelf Research, Volume 27, Issues 3–4, 2007, Pages 296-308, ISSN 0278-4343, https://doi.org/10.1016/j.csr.2005.08.029.

- Tesi T., Miserocchi S., Acri F., Langone L., Boldrin A., Hatten J. A., Albertazzi S., Flood-driven transport of sediment, particulate organic matter, and nutrients from the Po River watershed to the Mediterranean Sea, Journal of Hydrology, Volume 498, 2013, Pages 144-152, ISSN 0022-1694, https://doi.org/10.1016/j.jhydrol.2013.06.001.
- Van Rompaey A., Bazzoffi P., Jones R. J. A., Montanarella L., Modeling sediment yields in Italian catchments, Geomorphology, Volume 65, Issues 1–2, 2005, Pages 157-169, ISSN 0169-555X, https://doi.org/10.1016/j.geomorph.2004.08.006.
- Vázquez-Tarrío D., Ruiz-Villanueva V., Garrote J., Benito G., Calle M., Lucía A., & Díez-Herrero A. (2024). Effects of sediment transport on flood hazards: Lessons learned and remaining challenges. Geomorphology, 446, 108976.
- Vercruysse K., Grabowski Robert C., Rickson R.J., Suspended sediment transport dynamics in rivers: Multi-scale drivers of temporal variation, Earth-Science Reviews, Volume 166, 2017, Pages 38-52, ISSN 0012-8252.
- Vignati D., Pardos M., Diserens J., Ugazio G., Thomas R., Dominik J., Characterisation of bed sediments and suspension of the river Po (Italy) during normal and high flow conditions, Water Research, Volume 37, Issue 12, 2003, Pages 2847-2864, ISSN 0043-1354, https://doi.org/10.1016/S0043-1354(03)00133-7.
- Walker D. B., Brusseau M. L., Fitzsimmons K., 2003, Physical-chemical characteristics of water, chapter 3, University of Arizona. https://cales.arizona.edu/limnology/20229%20ch%2003.pdf
- Wilkes M. A., Gittins J.R., Mathers K.L., et al. Physical and biological controls on fine sediment transport and storage in rivers. *WIREs Water*. 2019; 6:e1331. https://doi.org/10.1002/wat2.1331
- Yang S., Zhao Q.-Y., Belkin I. M., Temporal variation in the sediment load of the Yangtze river and the influences of human activities, Journal of Hydrology, Volume 263, Issues 1–4, 2002, Pages 56-71, ISSN 0022-1694, https://doi.org/10.1016/S0022-1694(02)00028-8.
- Yokoo Y. and Sivapalan M.: Towards reconstruction of the flow duration curve: development of a conceptual framework with a physical basis, Hydrol. Earth Syst. Sci., 15, 2805–2819, https://doi.org/10.5194/hess-15-2805-2011, 2011

- Zanchettin, D., Traverso, P. & Tomasino, M. (2008) Po River discharges: a preliminary analysis of a 200-year time series. Climatic Change, 89(3), 411–433. Available from: https://doi.org/10.1007/s10584-008- 9395-z
- Zhao W., Guan X., Zhang Z., Wang Z., Wang L., Mamer E. A., Development of flow-duration-frequency curves for episodic low streamflow, Advances in Water Resources, Volume 156, 2021, 104021, ISSN 0309-1708, https://doi.org/10.1016/j.advwatres.2021.104021.